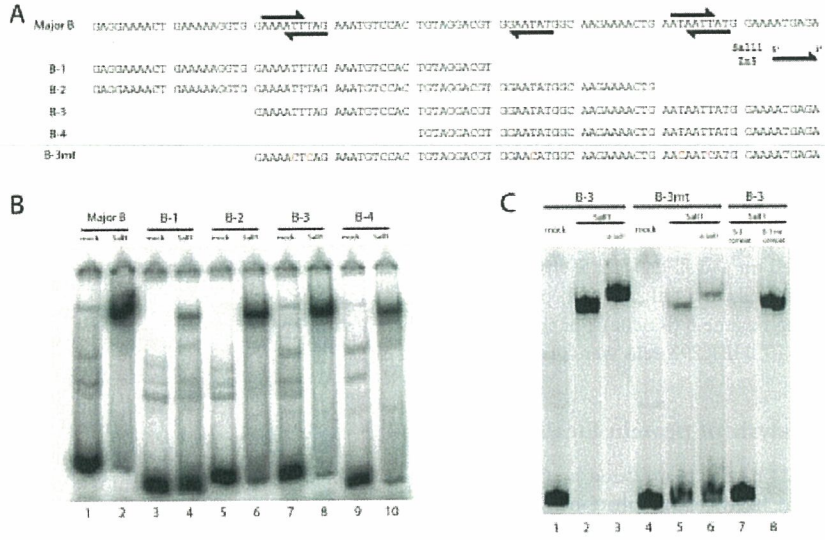

Figure 7 Sall1 recognizes the AT-rich sequences of major satellite DNA. (A) Major B deletion and mutant probes. The arrows indicate A/T-rich sequences similar to the Sall1 Zn5 consensus sequences (5′→3′). The positions of the point mutations are shown in red. (B) EMSAs using Major B deletion mutants. (C) EMSAs showing the affinity attenuation for B-3mt (lanes 1–6). Excess amounts of non-labeled B-3 and B-3mt were added to show the binding specificity (lanes 7 and 8, respectively).

involved in the formation or maintenance of heterochromatin. Sall1 was reported to associate with HDAC and several components of the NuRD chromatin remodeling complex (MTA1, MTA2 and RbAp46/48) (Kiefer *et al.* 2002; Lauberth & Rauchman 2006). By binding to the major satellite DNA and recruiting these remodeling factors to heterochromatin, Sall1 could participate in the formation or maintenance of chemical modifications of histones or DNA in heterochromatin. Alternatively, Sall1 may function as a transcriptional regulator similar to Ikaros, another C2H2 zinc finger protein that also localizes to heterochromatin and associates with major satellite DNA. Sall1, as well as Ikaros, may regulate gene expression by repositioning target gene loci to heterochromatin (Brown *et al.* 1997; Cobb *et al.* 2000; Koipally *et al.* 2002). To test this hypothesis, it is necessary to identify the direct downstream targets and demonstrate the association of these loci with Sall1. Recently, it was reported that Sall4, in cooperation with Tbx5, up-regulates *Fgf10* in developing forelimbs and both up-regulates *Gja5* and down-regulates *Nppa* in the developing heart (Koshiba-Takeuchi *et al.* 2006). In zebrafish, *sall1a*, the ortholog of *Sall1*, functions with *sall4* and regulates *fgfr2* and *fgf10* expressions in pectoral fin development (Harvey & Logan 2006). Thus it is necessary to test whether the gene loci of *Fgf10* and other potential Sall1 targets in mammals are associated with heterochromatin. Finally, Sall1 may bind to A/T-rich sequences in the promoter region of target genes that do not associate with heterochromatin. Although our data suggest that this is less likely, it remains possible that a small amount of Sall1 protein exists in non-heterochromatic regions and regulates gene expression as a transcription factor. In any case, it is necessary to identify the direct target genes of Sall1 and the molecules it associates with. Taken together, our data have revealed the heterochromatin localization mechanism of Sall1, and further elucidation of Sall1 functions at this site would lead to better understanding of organ development and the mechanisms of Townes–Brocks syndrome.

Experimental procedures

Plasmids

A Sall1-GFP expression vector (pCAGEN-Sall1-GFP) and N-terminal HA-tagged Sall1 expression vector (pCAGEN-HA-Sall1) were produced as described previously (Sato *et al.* 2004) from pCAGEN, a mammalian expression vector driven by the CAG promoter (Niwa *et al.* 1991). Sall1 zinc finger mutants were produced by replacing each of the zinc finger clusters of pCAGEN-Sall1-GFP with mutated fragments. Site-directed mutagenesis was performed by PCR using a Sall1 cDNA as a template and primers designed to alter the cysteine residues of each zinc finger to glycine, producing Zn1-5mut. In α-helix Zn2-5 mut, α-helix amino acids were changed to the Sall2 form. All PCR reactions were carried out using *Pfu* DNA polymerase (Promega). Each zinc finger mutant fragment amplified by PCR was cloned into pCR-Blunt II-TOPO (Invitrogen) and verified by sequencing. The Zn1 point mutant fragment was excised by *EcoRI* digestion, the Zn2 mutant by *SacI* and *ApaI* digestion, the Zn3 mutant by *ApaI* and *XhoI* digestion, the Zn4 mutant by *XhoI* and *SpeI* digestion and the Zn5 mutant by *SpeI* and *AgeI* digestion, followed by in-frame replacement of wild-type Sall1 with each mutant fragment. pCAGEN-HA-tagged Zn2-5mut, Zn23mut and Zn45mut without GFP, which were used for EMSAs, were generated by replacing the *EcoRI-SfiI* fragment of pCAGEN-HA-Sall1 with fragments of pCAGEN-Zn2-5mut-GFP, pCAGEN-Zn23mut-GFP and pCAGEN-Zn45mut-GFP, respectively.

To generate a GST-Zn5 bacterial expression vector, the *SpeI-NotI* fragment of Sall1 cDNA (Sato *et al.* 2004) was inserted in-frame into the *SmaI* site of pGEX-4T-3 (GE Healthcare).

Cell culture and transfection

For immunocytochemistry, E14.1 ES cells were plated on 4-well Lab-TekII chamber slides (Nunc) at a density of 5×10^3 cells/well. For localization of GFP-fused Sall1 mutants, NIH3T3 cells were plated on 4-well Lab-TekII chamber slides at a density of 1×10^4 cells/well, and 1 μg of each plasmid was transiently introduced using Fugene 6 (Roche). For the nuclear extracts used in EMSAs, 3×10^6 HEK293 cells were plated in 100-mm dishes.

Analysis of protein localization in cells

At 24 h after transfection of GFP-fused mutants, NIH3T3 cells were fixed in phosphate-buffered saline (PBS) containing 2% paraformaldehyde, 0.1% Triton X-100 and 2 μg/mL DAPI at 4 °C for 20 min, and then washed for 3 × 5 min in PBS at room temperature. For immunocytochemistry, we used a monoclonal anti-Sall1 antibody (Sato *et al.* 2004), an anti-HP1α antibody (Catalog No. 07-346; Upstate Biotechnology) and an anti-tri-methylated H3K9 antibody (Catalog No. 07-523; Upstate Biotechnology). After fixation, the cells were blocked with 10% goat serum for 30 min at room temperature, incubated with each primary antibody diluted 1 : 100 in PBS containing 1% goat serum for 1 h at room temperature, rinsed with PBS and detected using an Alexa Fluor 488-conjugated anti-mouse IgG secondary antibody (Molecular Probes) or rhodamine-conjugated anti-rabbit IgG secondary antibody (Chemicon). The localization of the labeled proteins was detected using a confocal microscope (Radiance 2100; Bio-Rad).

Binding site selection

For binding site selection, we employed the CASTing technique as previously described (Morinaga *et al.* 2005) with some modifications. Single-stranded oligonucleotides containing a 20-bp random sequence flanked by a 20-bp PCR primer annealing site were synthesized (5′-GCTCTGGAACTAGTGAGTCC-N20-CGATTCTGTCGACCTCGAAG-3′). A dsDNA library was generated via extension by Taq polymerase primed with a reverse primer (5′-CTTCGAGGTCGACAGAATCG-3′). An aliquot (2 ng) of the dsDNA library was mixed with an excess of GST-Zn5 bound to glutathione-Sepharose beads (GE Healthcare) in 100 μL of CASTing binding buffer (20 mM Tris–HCl pH 8.0, 150 mM NaCl, 2 mM $MgCl_2$, 25 μM $ZnCl_2$, 0.2 mM EDTA, 10% glycerol, 0.1% NP-40, 1 mM dithiothreitol (DTT), 1 mg/mL bovine serum albumin (BSA), 100 μg/μL poly[dI-dC] and 1% (v/v) protease inhibitor cocktail for mammalian cell extracts (Sigma)) and incubated at 4 °C for 30 min with continual rotation. After six washes with binding buffer (without BSA or poly[dI-dC]), the DNA-protein complexes were eluted by incubating the beads with elution buffer (5 mM reduced glutathione, 100 mM Tris–HCl pH 8.0 and 150 mM NaCl). Selected oligonucleotides were recovered by phenol extraction and ethanol precipitation, and amplified by 20 cycles of PCR with a forward primer (5′-GCTCTGGAACTAGTGAGTCC-3′) and the above-described reverse primer. The same procedure was repeated for three additional rounds using 15 cycles of PCR for each. The final PCR products were subcloned into pCRII-TOPO (Invitrogen) and sequenced.

EMSAs

Bacterially-expressed GST-Zn5 was purified from bacterial lysates by binding to glutathione-Sepharose beads, followed by competitive elution with reduced glutathione. Aliquots (200 ng) of the protein were mixed with ^{32}P-labeled DNA probes (20 000 cpm) in 15 μL of CASTing binding buffer (without BSA), incubated at 30 °C for 30 min and then resolved by 4% polyacrylamide gel electrophoresis in 0.5 × TBE and 5% glycerol. The gels were dried and autoradiographed. To prepare ^{32}P-labeled probes, the final CASTing PCR products and dsDNA library before CASTing were labeled by PCR using [α-^{32}P]dCTP. Individual cloned sequences (probes 1, 2, 3, 4, 4-1 and 4-2) were excised from the cloned plasmids by *EcoRI* digestion, labeled using the Klenow large fragment (Takara) and [α-^{32}P]dATP, and purified using MicroSpin G-25 columns (GE Healthcare).

For nuclear extract preparation, HEK293 cells were transiently transfected with 6 μg of each plasmid. After 48 h, the cells were washed with PBS, lysed with 600 μL of buffer A (10 mM HEPES–KOH pH 7.8, 10 mM KCl, 1.5 mM $MgCl_2$, 0.05% NP-40, 0.5 mM DTT and 5% (v/v) protease inhibitor cocktail for mammalian cell extracts) for 10 min on ice and centrifuged at 2 300 *g* for 1 min. The pellet was suspended in 300 μL of buffer B (20 mM HEPES–KOH pH 7.8, 500 mM NaCl, 1.5 mM $MgCl_2$, 0.5 mM DTT and 5% v/v protease inhibitor cocktail for mammalian cell extracts), rotated at 4 °C for 30 min and centrifuged at 20 000 *g* for 30 min. The supernatant was diluted with an equal volume of buffer B containing 50% glycerol. The relative amount of each Sall1 protein was determined by Western blot analysis using the anti-Sall1 monoclonal antibody. The Sall1 protein level was normalized by dilution, with reference to nuclear extracts from cells transfected with the empty pCAG-EGFP vector.

The major satellite DNA probes were amplified by PCR using *Pfu* DNA polymerase, genomic DNA extracted from C57BL/6 mice and the following primers: Major satellite: forward, 5′-GGAATTCGGACCTGGAAATAGGCG-3′ and reverse, 5′-GGAATTCTTCAGTGTGCATTTCTCATTTTTCACG-3′; Major A:

forward, 5′-GAATTCGGACCTGGAAATAGGCGA-GAAAAC-3′ and

reverse, 5′-AGTTTTCCTCGCCATATTTCACGTCCTAAA-3′; Major B:

forward, 5′-GAGGAAAACTGAAAAAGGTGGAAAATT-TAG-3′ and

reverse, 5′-TCTCATTTTCCATAATTATTCAGTTTTCTT-3′; and Major C:

forward, 5′-GAAAATGAGAAACATCCACTTGAAGACTTG-3′ and

reverse, 5′-GAATTCTTCAGTGTGCATTTCTCATTT-3′.

Each fragment amplified by PCR was cloned into pCR-Blunt II-TOPO. Major B mutant fragments were derived from synthetic ds oligonucleotides and also cloned into pCR-Blunt II-TOPO.

For EMSAs, 3-μL aliquots of the nuclear extracts were diluted with 12 μL of EMSA reaction buffer (50 mM HEPES–KOH pH 7.8, 1.5 mM $MgCl_2$, 0.5 mM DTT, 0.05 mM $ZnCl_2$, 1% (v/v) protease inhibitor cocktail for mammalian cell extracts, 20% (v/v) glycerol, radioisotope-labeled probe (5×10^4 cpm)), incubated at 30 °C for 30 min, and then separated by polyacrylamide gel electrophoresis in 4% gels containing 15% glycerol with 0.5 ×TBE as the electrophoresis buffer.

Acknowledgements

We thank T. Morinaga, M. Takahashi and H. Yamazaki for technical advice, and T. Ishida, H. Iba, H. Watanabe and S. Ohno for helpful discussions. This work was supported in part by the Ministry of Education, Culture, Sports, Science and Technology of Japan and by the Ministry of Health, Labor and Welfare of Japan. Akira Sato was supported by the Japan Society for the Promotion of Science.

References

Al-Baradie, R., Yamada, K., St Hilaire, C., Chan, W.M., Andrews, C., McIntosh, N., Nakano, M., Martonyi, E.J., Raymond, W.R., Okumura, S., Okihiro, M.M. & Engle, E.C. (2002) Duane radial ray syndrome (Okihiro syndrome) maps to 20q13 and results from mutations in *SALL4*, a new member of the SAL family. *Am. J. Hum. Genet.* **71**, 1195–1199.

Barrio, R., Shea, M.J., Carulli, J., Kipkow, K., Gaul, U., Frommer, G., Schuh, R., Jackle, H. & Kafatos, F.C. (1996) The *spalt*-related gene of *Drosophila melanogaster* is a member of an ancient gene family, defined by the adjacent, region-specific homeotic gene spalt. *Dev. Genes Evol.* **206**, 315–325.

Borozdin, W., Steinmann, K., Albrecht, B., Bottani, A., Devriendt, K., Leipoldt, M. & Kohlhase, J. (2006) Detection of heterozygous *SALL1* deletions by quantitative real time PCR proves the contribution of a *SALL1* dosage effect in the pathogenesis of Townes–Brocks syndrome. *Hum. Mutat.* **27**, 211–212.

Boube, M., Llimargas, M. & Casanova, J. (2000) Cross-regulatory interactions among tracheal genes support a co-operative model for the induction of tracheal fates in the *Drosophila* embryo. *Mech. Dev.* **91**, 271–278.

Brown, K.E., Guest, S.S., Smale, S.T., Hahm, K., Merkenschlager, M. & Fisher, A.G. (1997) Association of transcriptionally silent genes with Ikaros complexes at centromeric heterochromatin. *Cell* **91**, 845–854.

Buck, A., Archangelo, L., Dixkens, C. & Kohlhase, J. (2000) Molecular cloning, chromosomal localization, and expression of the murine SALL1 ortholog *Sall1*. *Cytogenet. Cell Genet.* **89**, 150–153.

Buck, A., Kispert, A. & Kohlhase, J. (2001) Embryonic expression of the murine homologue of *SALL1*, the gene mutated in Townes–Brocks syndrome. *Mech. Dev.* **104**, 143–146.

de Celis, J.F. & Barrio, R. (2000) Function of the *spalt/spalt-related* gene complex in positioning the veins in the *Drosophila* wing. *Mech. Dev.* **91**, 31–41.

de Celis, J.F., Barrio, R. & Kafatos, F.C. (1996) A gene complex acting downstream of *dpp* in *Drosophila* wing morphogenesis. *Nature* **381**, 421–424.

Cobb, B.S., Morales-Alcelay, S., Kleiger, G., Brown, K.E., Fisher, A.G. & Smale, S.T. (2000) Targeting of Ikaros to pericentromeric heterochromatin by direct DNA binding. *Genes Dev.* **14**, 2146–2160.

Dong, P.D., Todi, S.V., Eberl, D.F. & Boekhoff-Falk, G. (2003) *Drosophila spalt/spalt-related* mutants exhibit Townes–Brocks' syndrome phenotypes. *Proc. Natl. Acad. Sci. USA* **100**, 10293–10298.

Elstob, P.R., Brodu, V. & Gould, A.P. (2001) *spalt*-dependent switching between two cell fates that are induced by the *Drosophila* EGF receptor. *Development* **128**, 723–732.

Harvey, S.A. & Logan, M.P. (2006) *sall4* acts downstream of *tbx5* and is required for pectoral fin outgrowth. *Development* **113**, 1165–1173.

Horz, W. & Altenburger, W. (1981) Nucleotide sequence of mouse satellite DNA. *Nucleic Acids Res.* **9**, 683–696.

Kiefer, S.M., McDill, B.W., Yang, J. & Rauchman, M. (2002) Murine Sall1 represses transcription by recruiting a histone deacetylase complex. *J. Biol. Chem.* **277**, 14869–14876.

Kiefer, S.M., Ohlemiller, K.K., Yang, J., McDill, B.W., Kohlhase, J. & Rauchman, M. (2003) Expression of a truncated Sall1 transcriptional repressor is responsible for Townes–Brocks syndrome birth defects. *Hum. Mol. Genet.* **12**, 2221–2227.

Kohlhase, J. (2000) *SALL1* mutations in Townes–Brocks syndrome and related disorders. *Hum. Mutat.* **16**, 460–466.

Kohlhase, J., Altmann, M., Archangelo, L., Dixkens, C. & Engel, W. (2000) Genomic cloning, chromosomal mapping, and expression analysis of *msal-2*. *Mamm. Genome* **11**, 64–68.

Kohlhase, J., Hausmann, S., Stojmenovic, G., Dixkens, C., Bink, K., Schulz-Schaeffer, W., Altmann, M. & Engel, W. (1999) *SALL3*, a new member of the human *spalt*-like gene family, maps to 18q23. *Genomics* **62**, 216–222.

Kohlhase, J., Heinrich, M., Liebers, M., Frohlich Archangelo, L., Reardon, W. & Kispert, A. (2002a) Cloning and expression analysis of *Sall4*, the murine homologue of the gene mutated in Okihiro syndrome. *Cytogenet. Genome Res.* **98**, 274–277.

Kohlhase, J., Heinrich, M., Schubert, L., Liebers, M., Kispert, A., Laccone, F., Turnpenny, P., Winter, R.M. & Reardon, W. (2002b) Okihiro syndrome is caused by *SALL4* mutations. *Hum. Mol. Genet.* **11**, 2979–2987.

Kohlhase, J., Schuh, R., Dowe, G., Kuhnlein, R.P., Jackle, H., Schroeder, B., Schulz-Schaeffer, W., Kretzschmar, H.A., Kohler, A., Muller, U., Raab-Vetter, M., Burkhardt, E., Engel, W. & Stick, R. (1996) Isolation, characterization, and organ-specific expression of two novel human zinc finger genes related to the *Drosophila* gene *spalt*. *Genomics* **38**, 291–298.

Kohlhase, J., Wischermann, A., Reichenbach, H., Froster, U. & Engel, W. (1998) Mutations in the *SALL1* putative transcription factor gene cause Townes–Brocks syndrome. *Nat. Genet.* **18**, 81–83.

Koipally, J., Heller, E.J., Seavitt, J.R. & Georgopoulos, K. (2002) Unconventional potentiation of gene expression by Ikaros. *J. Biol. Chem.* **277**, 13007–13015.

Koshiba-Takeuchi, K., Takeuchi, J.K., Arruda, E.P., Kathiriya, I.S., Mo, R., Hui, C.C., Srivastava, D. & Bruneau, B.G. (2006) Cooperative and antagonistic interactions between Sall4

and Tbx5 pattern the mouse limb and heart. *Nat. Genet.* **38**, 175–183.

Lachner, M., O'Sullivan, R.J. & Jenuwein, T. (2003) An epigenetic road map for histone lysine methylation. *J. Cell Sci.* **116**, 2117–2124.

Lauberth, S.M. & Rauchman, M. (2006) A conserved 12-amino acid motif in Sall1 recruits the nucleosome remodeling and deacetylase corepressor complex. *J. Biol. Chem.* **281**, 23922–23931.

Mollereau, B., Dominguez, M., Webel, R., Colley, N.J., Keung, B., de Celis, J.F. & Desplan, C. (2001) Two-step process for photoreceptor formation in *Drosophila*. *Nature* **412**, 911–913.

Morinaga, T., Enomoto, A., Shimono, Y., Hirose, F., Fukuda, N., Dambara, A., Jijiwa, M., Kawai, K., Hashimoto, K., Ichihara, M., Asai, N., Murakumo, Y., Matsuo, S. & Takahashi, M. (2005) GDNF-inducible zinc finger protein 1 is a sequence-specific transcriptional repressor that binds to the *HOXA10* gene regulatory region. *Nucleic Acids Res.* **33**, 4191–4201.

Netzer, C., Bohlander, S.K., Hinzke, M., Chen, Y. & Kohlhase, J. (2006) Defining the heterochromatin localization and repression domains of SALL1. *Biochim. Biophys. Acta* **1762**, 386–391.

Netzer, C., Rieger, L., Brero, A., Zhang, C.D., Hinzke, M., Kohlhase, J. & Bohlander, S.K. (2001) *SALL1*, the gene mutated in Townes–Brocks syndrome, encodes a transcriptional repressor which interacts with TRF1/PIN2 and localizes to pericentromeric heterochromatin. *Hum. Mol. Genet.* **10**, 3017–3024.

Nielsen, A.L., Oulad-Abdelghani, M., Ortiz, J.A., Remboutsika, E., Chambon, P. & Losson, R. (2001) Heterochromatin formation in mammalian cells: interaction between histones and HP1 proteins. *Mol. Cell* **7**, 729–739.

Nishinakamura, R., Matsumoto, Y., Nakao, K., Nakamura, K., Sato, A., Copeland, N.G., Gilbert, D.J., Jenkins, N.A., Scully, S., Lacey, D.L., Katsuki, M., Asashima, M. & Yokota, T. (2001) Murine homolog of *SALL1* is essential for ureteric bud invasion in kidney development. *Development* **128**, 3105–3115.

Niwa, H., Yamamura, K. & Miyazaki, J. (1991) Efficient selection for high-expression transfectants with a novel eukaryotic vector. *Gene* **108**, 193–199.

Ott, T., Kaestner, K.H., Monaghan, A.P. & Schutz, G. (1996) The mouse homolog of the region specific homeotic gene spalt of *Drosophila* is expressed in the developing nervous system and in mesoderm-derived structures. *Mech. Dev.* **56**, 117–128.

Ott, T., Parrish, M., Bond, K., Schwaeger-Nickolenko, A. & Monaghan, A.P. (2001) A new member of the spalt like zinc finger protein family, Msal-3, is expressed in the CNS and sites of epithelial/mesenchymal interaction. *Mech. Dev.* **101**, 203–207.

Pabo, C.O., Peisach, E. & Grant, R.A. (2001) Design and selection of novel Cys2His2 zinc finger proteins. *Annu. Rev. Biochem.* **70**, 313–340.

Peters, A.H., Kubicek, S., Mechtler, K., O'Sullivan, R.J., Derijck, A.A., Perez-Burgos, L., Kohlmaier, A., Opravil, S., Tachibana, M., Shinkai, Y., Martens, J.H. & Jenuwein, T. (2003) Partitioning and plasticity of repressive histone methylation states in mammalian chromatin. *Mol. Cell* **12**, 1577–1589.

Reuter, D., Schuh, R. & Jackle, H. (1989) The homeotic gene spalt (*sal*) evolved during *Drosophila* speciation. *Proc. Natl. Acad. Sci. USA* **86**, 5483–5486.

Rusten, T.E., Cantera, R., Urban, J., Technau, G., Kafatos, F.C. & Barrio, R. (2001) Spalt modifies EGFR-mediated induction of chordotonal precursors in the embryonic PNS of *Drosophila* promoting the development of oenocytes. *Development* **128**, 711–722.

Sakaki-Yumoto, M., Kobayashi, C., Sato, A., Fujimura, S., Matsumoto, Y., Takasato, M., Kodama, T., Aburatani, H., Asashima, M., Yoshida, N. & Nishinakamura, R. (2006) The murine homolog of *SALL4*, a causative gene in Okihiro syndrome, is essential or embryonic stem cell proliferation, and cooperates with *Sall1* in anorectal, heart, brain and kidney development. *Development* **133**, 3005–3013.

Sato, A., Kishida, S., Tanaka, T., Kikuchi, A., Kodama, T., Asashima, M. & Nishinakamura, R. (2004) Sall1, a causative gene for Townes–Brocks syndrome, enhances the canonical Wnt signaling by localizing to heterochromatin. *Biochem. Biophys. Res. Commun.* **319**, 103–113.

Sato, A., Matsumoto, Y., Koide, U., Kataoka, Y., Yoshida, N., Yokota, T., Asashima, M. & Nishinakamura, R. (2003) Zinc finger protein Sall2 is not essential for embryonic and kidney development. *Mol. Cell. Biol.* **23**, 62–69.

Sweetman, D., Smith, T., Farrell, E.R., Chantry, A. & Munsterberg, A. (2003) The conserved glutamine-rich region of chick csal1 and csal3 mediates protein interactions with other spalt family members. Implications for Townes–Brocks syndrome. *J. Biol. Chem.* **278**, 6560–6566.

Wong, A.K. & Rattner, J.B. (1988) Sequence organization and cytological localization of the minor satellite of mouse. *Nucleic Acids Res.* **16**, 11645–11661.

Wright, W.E., Binder, M. & Funk, W. (1991) Cyclic amplification and selection of targets (CASTing) for the myogenin consensus binding site. *Mol. Cell. Biol.* **11**, 4104–4110.

Received: 26 April 2006
Accepted: 30 Oct 2006

ELSEVIER

Mechanisms of Development 124 (2007) 290–303

www.elsevier.com/locate/modo

Six1 and *Six4* are essential for *Gdnf* expression in the metanephric mesenchyme and ureteric bud formation, while *Six1* deficiency alone causes mesonephric-tubule defects

Hiroki Kobayashi [a,b], Kiyoshi Kawakami [c], Makoto Asashima [d,e], Ryuichi Nishinakamura [a,*]

[a] *Division of Integrative Cell Biology, Institute of Molecular Embryology and Genetics, Kumamoto University, 2-2-1 Honjo, Kumamoto 860-0811, Japan*
[b] *Department of Biological Sciences, Graduate School of Science, The University of Tokyo, Tokyo, Japan*
[c] *Division of Biology, Center for Molecular Medicine, Jichi Medical University, Tochigi, Japan*
[d] *Department of Life Sciences (Biology), Graduate School of Arts and Sciences, The University of Tokyo, Tokyo, Japan*
[e] *International Cooperative Research Project (ICORP), Japan Science and Technology Agency (JST), Tokyo, Japan*

Received 21 August 2006; received in revised form 24 December 2006; accepted 5 January 2007
Available online 11 January 2007

Abstract

Interaction between the ureteric-bud epithelium and the metanephric mesenchyme is important for kidney development. *Six1* and *Six4* are the mammalian homologs of *Drosophila sine oculis*, and they are coexpressed in the nephrogenic mesenchyme. *Six1*-deficient mice show varying kidney defects, while *Six4*-deficient mice have no apparent abnormalities. Here, we report *Six1*/*Six4*-deficient mice that we generated in order to elucidate the functions of *Six4* in *Six1*-deficient kidney development. The *Six1*/*Six4*-deficient mice exhibited more severe kidney phenotypes than the *Six1*-deficient mice; kidney and ureter agenesis was observed in all the neonates examined. The *Six1*/*Six4*-deficient metanephric mesenchyme cells were directed toward kidney lineage but failed to express *Pax2*, *Pax8*, or *Gdnf*, whereas the expression of these genes was partially reduced or unchanged in the case of *Six1* deficiency. Thus, *Six4* cooperates with *Six1* in the metanephric mesenchyme to regulate the level of *Gdnf* expression; this could explain the absence of the ureteric bud in the *Six1*/*Six4*-deficient mice. In contrast, *Six1* deficiency alone caused defects in mesonephric-tubule formation, and these defects were not exacerbated in the *Six1*/*Six4*-deficient mesonephros. These results highlight the fact that *Six1* and *Six4* have collaborative functions in the metanephros but not in the mesonephros.

Keywords: *Six1*; *Six4*; Kidney development; *Sall1*; *Gdnf*; *Pax2*; *Pax8*

1. Introduction

In mammals, kidney development occurs in three successive steps – initial pronephros formation followed by mesonephros formation and finally, metanephros formation. In mice, development of the first kidney – the pronephros – is initiated between embryonic day 8.0 and 8.5 (E8.0–E8.5) by signals from the paraxial mesoderm and surface ectoderm. These signals induce the intermediate mesoderm to differentiate into the Wolffian duct (nephric duct). Next, the nephrogenic cord – the mesenchymal tissue – is induced at the ventral side of the Wolffian duct (Obara-Ishihara et al., 1999; Mauch et al., 2000; James and Schultheiss, 2003). The Wolffian duct and nephrogenic cord elongate caudally towards the cloaca, and the Wolffian duct converts the adjacent mesenchyme (nephrogenic cord) into mesonephric tubules between E9.0 and E11.0. When the Wolffian duct reaches the level of the developing

* Corresponding author. Tel.: +81 96 373 6615; fax: +81 96 373 6618.
E-mail address: ryuichi@kaiju.medic.kumamoto-u.ac.jp (R. Nishinakamura).

0925-4773/$ - see front matter © 2007 Elsevier Ltd. All rights reserved.
doi:10.1016/j.mod.2007.01.002

hindlimb at E10.0, the ureteric bud evaginates from the Wolffian duct and invades the surrounding metanephric mesenchyme, which is formed as a bulge at the caudal-most region of the nephrogenic cord. Subsequently, both the metanephric mesenchyme and ureteric bud undergo reciprocal inductive interactions to form the nephrons and collecting ducts of the metanephros – the third and the adult kidney (Grobstein, 1953; Saxen, 1987). Thus, the two mesenchymal tissues – the nephrogenic cord and metanephric mesenchyme – constitute the nephrogenic mesenchyme.

During metanephros development, the glial cell line-derived neurotrophic factor (Gdnf) secreted from the mesenchyme acts on the receptor tyrosine kinase Ret and its co-receptor Gfra1, both of which are expressed in the Wolffian duct, and it induces ureteric-bud formation from the Wolffian duct. Thus, mice that are deficient in *Gdnf*, *Ret*, or *Gfra1* show similar phenotypes such as failure of ureteric-bud invasion into the mesenchyme (Durbec et al., 1996; Moore et al., 1996; Pichel et al., 1996; Sanchez et al., 1996; Sainio et al., 1997b; Cacalano et al., 1998; Enomoto et al., 1998; Sariola and Saarma, 1999). Several mesenchymal transcription factors also play important roles in metanephros formation (reviewed by Vainio and Lin, 2002). *Pax2* is expressed both in the metanephric mesenchyme and ureteric-bud, and *Pax2*-deficient mice show a reduced mesenchyme and failure in ureteric-bud invasion (Torres et al., 1995). *Pax2* has been shown to bind the *Gdnf* promoter, and this may explain the reduced *Gdnf* expression and the ureteric-bud phenotype in the mutant mice (Brophy et al., 2001). *Sall1* is expressed exclusively in the mesenchyme, and mice lacking this gene show phenotypes similar to those of *Pax2*-null mice (Nishinakamura et al., 2001). However, *Gdnf* and *Pax2* expression remains unaffected in *Sall1*-deficient mice, while *Sall1* continues to be expressed in *Pax2*-mutant mice. This suggests that *Sall1* may function independent of the *Pax2–Gdnf* pathway. *Wt1*-deficient mice also exhibit similar phenotypes; however, *Gdnf* expression is not affected in these mice (Kreidberg et al., 1993; Sainio et al., 1997b). Mice lacking *Osr1* do not develop the metanephric mesenchyme, and they do not express *Pax2*, *Gdnf*, or *Sall1*; this implies that *Osr1* is one of the most upstream genes in the metanephric cascade (James and Schultheiss, 2005; Wang et al., 2005; James et al., 2006).

The mesonephros comprises the mesonephric tubules and the Wolffian duct. Two types of mesonephric tubules are formed along the Wolffian duct. The first type comprises a few pairs of cranial mesonephric tubules, which develop as outgrowths from the Wolffian duct and later become epididymal ducts in males. The other type comprises caudal mesonephric tubules, which constitute a majority of the tubules and are formed in the nephrogenic cord – a mesenchymal tissue – upon induction by the Wolffian duct (Sainio et al., 1997a). Further, some of the genes involved in metanephros formation also play important roles in mesonephros development. *Pax2*-deficient mice show defects in mesonephric-tubule formation and Wolffian-duct elongation (Torres et al., 1995). *Wt1*-deficient mice lack the caudal mesonephric tubules but not the cranial tubules (Kreidberg et al., 1993; Sainio et al., 1997a). *Osr1* deficiency leads to asymmetric defects in Wolffian-duct elongation and to failure in mesonephric-tubule formation (James and Schultheiss, 2005; Wang et al., 2005; James et al., 2006). In contrast to these genes that are expressed in the nephrogenic cord (and also in the Wolffian duct in the case of *Pax2*), *Wnt9b* is expressed exclusively in the Wolffian duct and induces the nephrogenic cord to transform into mesonephric-tubule epithelia. Thus, *Wnt9b*-deficient mice lack mesonephric tubules (Carroll et al., 2005).

The initial specification toward the nephrogenic lineage from the intermediate mesoderm is beginning to be elucidated. *Pax2* and *Pax8* are coexpressed in the Wolffian duct and in the pro- and mesonephric tubules, and *Pax2/Pax8*-deficient mice exhibit complete absence of the pro-, meso-, and metanephros (Bouchard et al., 2002), suggesting redundant roles of the two transcription factors in kidney-lineage commitment. The homeodomain protein Lim1 is expressed early in the intermediate mesoderm, Wolffian duct, and pro- and mesonephric tubules (Fujii et al., 1994), and is required for kidney development (Kobayashi et al., 2005). In *Lim1*-deficient mice, the intermediate mesoderm is disorganized and fails to express *Pax2* – a prerequisite for kidney development (Tsang et al., 2000).

The *Six* homeobox genes are characterized by conserved six domains and a homeodomain, both of which are required for specific DNA binding. This gene family is essential for compound-eye development, and the prototype of this gene family is *Drosophila sine oculis*. Six members (*Six1–Six6*) of the *Six* gene family have been identified in mice and humans (Kawakami et al., 2000). *Six3* and *Six6* are essential for forebrain formation and eye development (Kobayashi et al., 1998; Loosli et al., 1999; Zuber et al., 1999; Carl et al., 2002; Zhu et al., 2002; Lagutin et al., 2003; Lopez-Rios et al., 2003), whereas *Six5* is involved in cataractogenesis and spermatogenesis (Sarkar et al., 2000, 2004). Several papers, including ours, report that *Six1*-deficient mice show anomalies in the development of various organs such as the inner ear, nose, thymus, kidney, and skeletal muscle (Laclef et al., 2003a,b; Zheng et al., 2003; Ozaki et al., 2004; Zou et al., 2004, 2006). During renal development, *Six1* is required for ureteric-bud invasion into the metanephric mesenchyme although variation among animals exists. In *Six1* deficiency, the metanephric mesenchyme is formed, although it is small. Further, expression of *Sall1* and *Six2* is absent, while that of *Pax2* and *Gdnf* is only partially reduced in this condition (Li et al., 2003; Xu et al., 2003). *Eya1*, a murine homolog of the *Drosophila eyes absent* gene, functions as a coactivator of the *Six* family genes. *Eya1*-deficient mice exhibit more severe kidney phenotypes than *Six1*-null mice – absence of the metanephric mesenchyme and ureteric-bud and complete reduction in the expression levels of *Pax2* and *Gdnf* (Xu et al., 1999; Nica et al., 2006). Thus, molecules other

than *Six1* that possibly cooperate with *Eya1* in kidney development might exist.

Six4, another member of the *Six* family, is separated from the *Six1* gene on the same chromosome by only 100 kb; its expression overlaps with that of *Six1* in many regions such as the neural placodes, Rathke's pouch, dorsal root ganglia, dermomyotome, myotome, limb bud mesenchyme, and myogenic migrating precursors (Grifone et al., 2005). Interestingly, as we previously demonstrated, *Six4*-deficient mice exhibit no major developmental defects and are fertile (Ozaki et al., 2001). Since Six1 and Six4 exhibited a similar binding specificity to the MEF3 site (TCAGGTTC), the roles played by *Six1* and *Six4* in embryogenesis may be redundant (Spitz et al., 1998; Himeda et al., 2004). The first evidence of this assumption was observed during myogenesis; *Six1* and *Six4* contribute to myogenic migration in somites by regulating *Pax3* and *Met* expression (Grifone et al., 2005). By independently generating *Six1/Six4*-deficient mice, we here demonstrate that these two transcription factors (*Six1* and *Six4*) have overlapping functions in kidney development. The *Six1/Six4*-deficient mice exhibited more severe kidney phenotypes than the *Six1*-deficient mice. The expression of *Pax2*, *Pax8*, and *Gdnf* was completely lost in the *Six1/Six4*-deficient metanephric mesenchyme, while it was partially reduced or unchanged in the *Six1*-deficient mice. These results indicate that *Six1* and *Six4* are required for metanephric mesenchyme development.

2. Results

2.1. Six1 and Six4 are coexpressed in the nephrogenic cord and metanephric mesenchyme

To demonstrate the overlapping expression patterns of *Six1* and *Six4* in the mesenchyme of developing renal tissues, we performed in situ hybridization for these two genes by using sections of E9.5 and E10.5 embryos, as described in Fig. 1A and B. In addition to its expression in somites (Oliver et al., 1995), *Six1* was expressed in the nephrogenic cord on E9.5 and in the metanephric mesenchyme on E10.5 but not expressed in the Wolffian duct (Fig. 1C–E). The domains of *Six4* expression were similar to those of *Six1*. *Six4* expression, although weak, was also detected in the nephrogenic cord and metanephric mesenchyme, both of which are mesenchymal components of the developing kidney (Fig. 1F–H).

2.2. Kidney phenotypes are exacerbated in Six1/Six4-deficient mice

Since *Six1* and *Six4* are on the same chromosome and closely linked, we introduced the *Six1*-targeting vector into *Six4*-heterozygous embryonic stem cells, and we generated strains with mutations in both the genes. As recently described in our paper, the resultant *Six1/Six4*-heterozygous mice appeared to be normal and fertile. Further, after heterozygous crossing, mice homozygous for *Six1* and *Six4* were born at the expected Mendelian frequency (Konishi et al., 2006). However, the *Six1/Six4*-deficient mice died soon after birth and showed developmental defects in various organs; this finding is consistent with a previous report (Grifone et al., 2005).

Further, by examining the kidney abnormalities in the *Six1/Six4*-deficient mice, we noted that they exhibited more severe phenotypes than the *Six1/Six4*-heterozygous or *Six1*-deficient mice. None of the *Six1/Six4*-heterozygous neonate mice showed developmental defects in the kidneys and ureters (Fig. 2A, Table 1). Of the *Six1*-deficient mice, 30% exhibited uni- or bilateral renal hypoplasia (Fig. 2B), and the remaining 70% exhibited kidney agenesis and had short ureters (Fig. 2C). In contrast, ureters and bilateral kidneys failed to develop in all the *Six1/Six4*-deficient mice, whereas the adrenal glands, urinary bladder, and genital tracts were formed without any apparent defects (Fig. 2D, Table 1).

Next, in the E11.5 embryos, we examined ureteric-bud invasion into the metanephric mesenchyme and the subsequent metanephric-mesenchyme condensation, an essential step for kidney and ureter formation. We stained the kidneys with an antibody against E-cadherin, which is expressed in the Wolffian duct and ureteric bud. A whole-mount view of the E-cadherin staining revealed that the ureteric bud originated from the Wolffian duct and branched in the *Six1/Six4*-heterozygous embryos (Fig. 2E). In the *Six1*-deficient embryos, the ureteric bud was formed but showed defects in elongation and branching (Fig. 2F and G). In contrast, ureteric-bud formation was never detected in the *Six1/Six4*-deficient embryos (Fig. 2H). Hematoxylin-eosin (HE)-stained sections of the E11.5 *Six1/Six4*-heterozygous embryos revealed no developmental defects in the invasion of the ureteric bud and condensation of the metanephric mesenchyme adjacent to the ureteric bud (Fig. 2I). In the *Six1*-deficient embryos, ureteric-bud invasion partially occurred, but variations were observed with regard to ureteric bud development and metanephric-mesenchyme condensation (Fig. 2J). In contrast, none of the *Six1/Six4*-deficient embryos showed ureteric-bud invasion and subsequent metanephric-mesenchyme condensation (Fig. 2K).

Further, prior to ureteric-bud invasion into the metanephric mesenchyme, we examined the metanephric mesenchyme at E10.5 by performing HE staining of the sections. The metanephric mesenchyme appeared as a distinct cell cluster adjacent to the Wolffian duct in the *Six1/Six4*-heterozygous (Fig. 2L and L′) and *Six1*-deficient embryos (Fig. 2M and M′), whereas this cell cluster was not observed in the *Six1/Six4*-deficient embryos (Fig. 2N and N′; arrowhead). Thus, the absence of *Six4* exacerbated *Six1*-deficient kidney phenotypes, suggesting that the transcription factors Six1 and Six4 cooperatively regulate the early stages of metanephros development and ureteric bud formation.

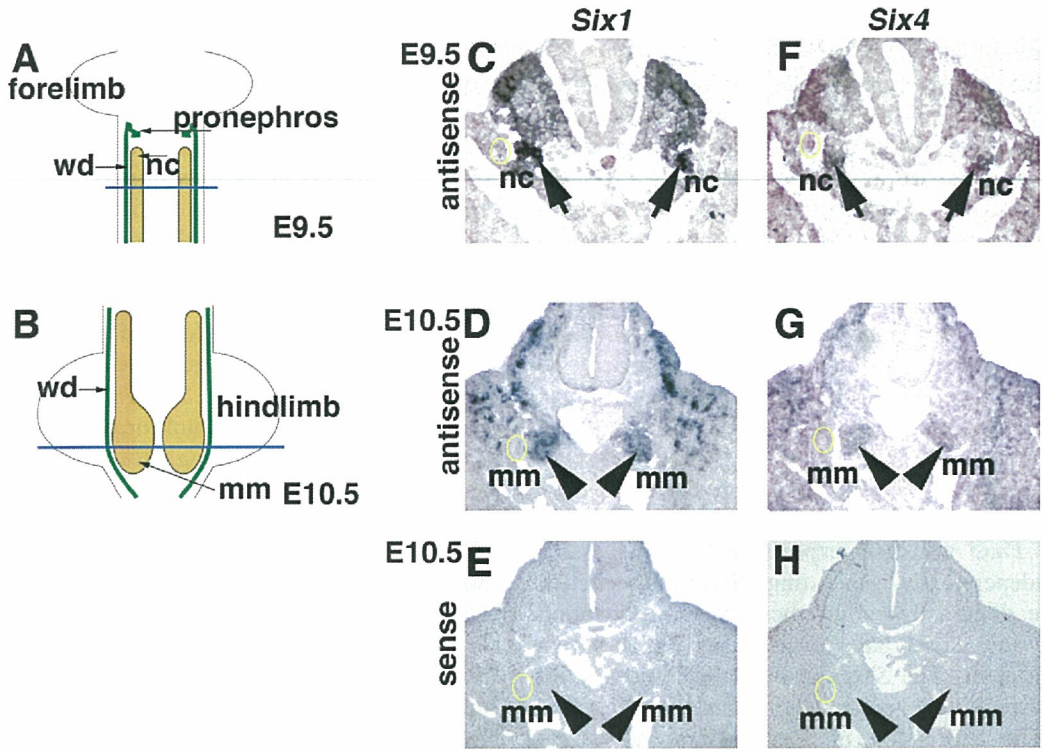

Fig. 1. Overlapping expression patterns of *Six1* and *Six4* in the nephrogenic mesenchyme. (A and B) Nephrogenic cord at E9.5 (A) and metanephric mesenchyme at E10.5 (B). Blue lines in A and B represent the planes along which the sections in C–H were sliced. (C–E) *Six1* expression in the developing kidneys in the E9.5 (C) and E10.5 (D) embryos. The sense probe produced no signals (E). (F–H) *Six4* expression in the developing kidneys in the E9.5 (F) and E10.5 (G) embryos. The sense probe produced no signals (H). *Six1* and *Six4* are coexpressed in the nephrogenic cord (arrow) in E9.5 embryos as well as in the metanephric mesenchyme (arrowhead) in the E10.5 embryos. The yellow circle indicates the Wolffian duct (nc, nephrogenic cord; mm, metanephric mesenchyme).

2.3. Pax2, Sall1, and Gdnf were absent in the Six1/Six4-deficient metanephric mesenchyme

To examine apoptosis, we carried out a TdT-mediated dUTP-digoxigenin nick end labeling (TUNEL) assay; however, apoptosis-positive cells were not detected in the metanephric mesenchyme of the *Six1/Six4*-heterozygous, *Six1*-deficient, or *Six1/Six4*-deficient embryos (Fig. 3A–C), suggesting that the absence of the mesenchymal cluster in *Six1/Six4* deficiency was not due to increased apoptosis in this region. Furthermore,expression of *EGFP* driven by the *Six1* locus (refer to Section 4), *Osr1*, and *Wt1*, which are known to be expressed at an early stage in kidney precursors (Kreidberg et al., 1993; James et al., 2006), was detected in the metanephric mesenchyme region of the *Six1/Six4*-deficient embryos as well as in the *Six1/Six4*-heterozygous and *Six1*-deficient embryos (Fig. 3D–L). This implied that the *Six1/Six4*-deficient metanephric mesenchymal cells were directed toward kidney lineage. In contrast, *Gdnf*, *Sall1*, and *Pax2* expression was severely affected in the *Six1/Six4*-deficient embryos. *Gdnf* was expressed in the metanephric mesenchyme in the *Six1/Six4*-heterozygous embryos (Fig. 3M), and it was weakly expressed in the *Six1*-deficient embryos (Fig. 3N). However, *Gdnf* expression was absent in the *Six1/Six4*-deficient embryos (Fig. 3O). These results are consistent with the complete absence of the ureteric bud in the *Six1/Six4*-deficient embryos and with its partial impairment in the *Six1*-deficient embryos because *Gdnf* is a critical regulator of ureteric budding. *Sall1* was expressed in the metanephric mesenchyme in the *Six1/Six4*-heterozygous embryos (Fig. 3P), but its expression was markedly lower in the *Six1*-deficient embryos and absent in the *Six1/Six4*-deficient embryos (Fig. 3Q and R). *Pax2* was expressed both in the metanephric mesenchyme and Wolffian duct in the *Six1/Six4*-heterozygous embryos (Fig. 3S). *Pax2* expression was lowered in the metanephric mesenchyme but not in the Wolffian duct in the *Six1*-deficient embryos, whereas it was completely absent in the *Six1/Six4*-deficient embryos (Fig. 3T and U). These results genetically place *Six1* and *Six4* downstream of *Osr1* and *Wt1* and upstream of *Gdnf*, *Sall1*, and *Pax2*. These results also imply that *Six1* and *Six4* redundantly regulate *Pax2* and *Gdnf* expression in the metanephric mesenchyme.

2.4. Six1 and Six4 regulate Pax8 in the metanephric mesenchyme

Together with *Pax2*, *Pax8* is also known to play a role in pro- and mesonephros development from the intermediate

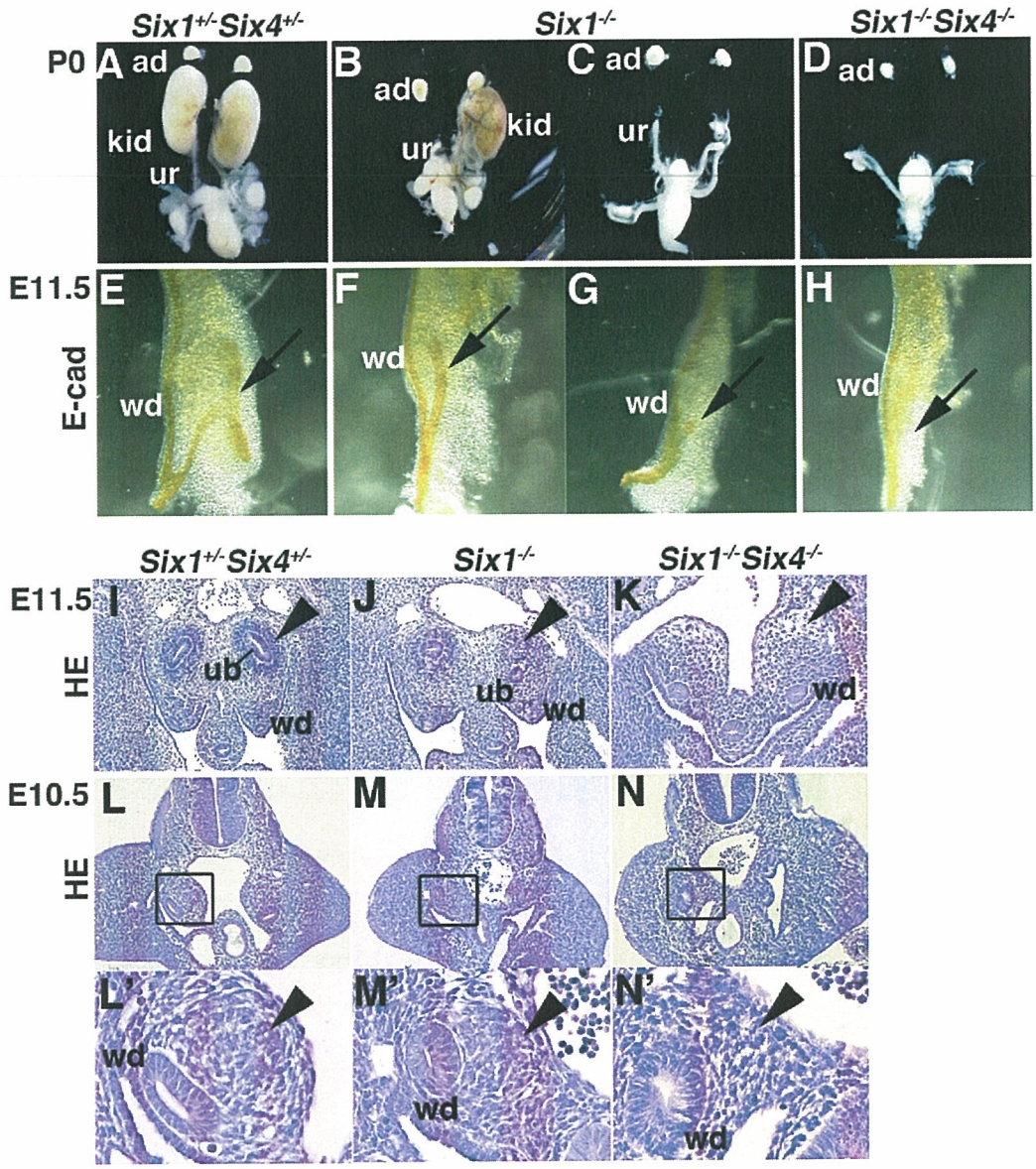

Fig. 2. *Six1*/*Six4*-deficient mice exhibit more severe renal defects than *Six1*-deficient mice. (A–D) Whole-mount views of urogenital tissues of the *Six1*/*Six4*-heterozygous (A), *Six1*-deficient (B and C), and *Six1*/*Six4*-deficient (D) newborn mice. Of the *Six1*-deficient mice, 30% exhibited uni- or bilateral renal hypoplasia (B) and the rest exhibited kidney agenesis (C). In contrast, all the *Six1*/*Six4*-deficient mice completely lacked kidney and ureter formation (D). (E–H) Whole-mount views of E-cadherin staining in the metanephric region of the E11.5 *Six1*/*Six4*- heterozygous (E), *Six1*-deficient (F and G), and *Six1*/*Six4*-deficient (H) embryos. The ureteric buds (arrow) were short and unbranched in the *Six1*-deficient embryos, while they were absent in the *Six1*/*Six4*-deficient embryos. (I–K) HE staining of the metanephric region of the E11.5 *Six1*/*Six4*-heterozygous (I), *Six1*-deficient (J), and *Six1*/*Six4*-deficient (K) embryos. The condensed mesenchyme (black arrowhead) was reduced, and the invasion of the ureteric bud into the mesenchyme was partially impaired in the *Six1*-deficient embryos (J). The mesenchymal cell cluster and the ureteric bud were not detected in the *Six1*/*Six4*-deficient embryos (K). (L–N) HE staining of the metanephric region of the E10.5 *Six1*/*Six4*-heterozygous (L), *Six1*-deficient (M), and *Six1*/*Six4*-deficient (N) embryos. (L′–N′) The lower panels are at a higher magnification than the upper panels (L–N). The mesenchymal cell cluster (arrowhead) was not detected in the *Six1*/*Six4*-deficient embryos (kid, kidney; ur, ureter; ad, adrenal gland; wd, Wolffian duct; ub, ureteric bud).

Table 1
Kidney abnormalities in newborn mutants

Genotype	Normal kidney	Hypoplastic kidney[a]	Kidney agenesis[b]	Kidney & ureter agenesis
Six1$^{+/-}$*Six4*$^{+/-}$	8/8	0/8	0/8	0/8
Six1$^{-/-}$	0/20	6/20	14/20	0/20
Six1$^{-/-}$*Six4*$^{-/-}$	0/15	0/15	0/15	15/15

[a] Bilateral hypoplastic kidneys or unilateral agenesis.
[b] A lack of bilateral kidneys but not ureters.

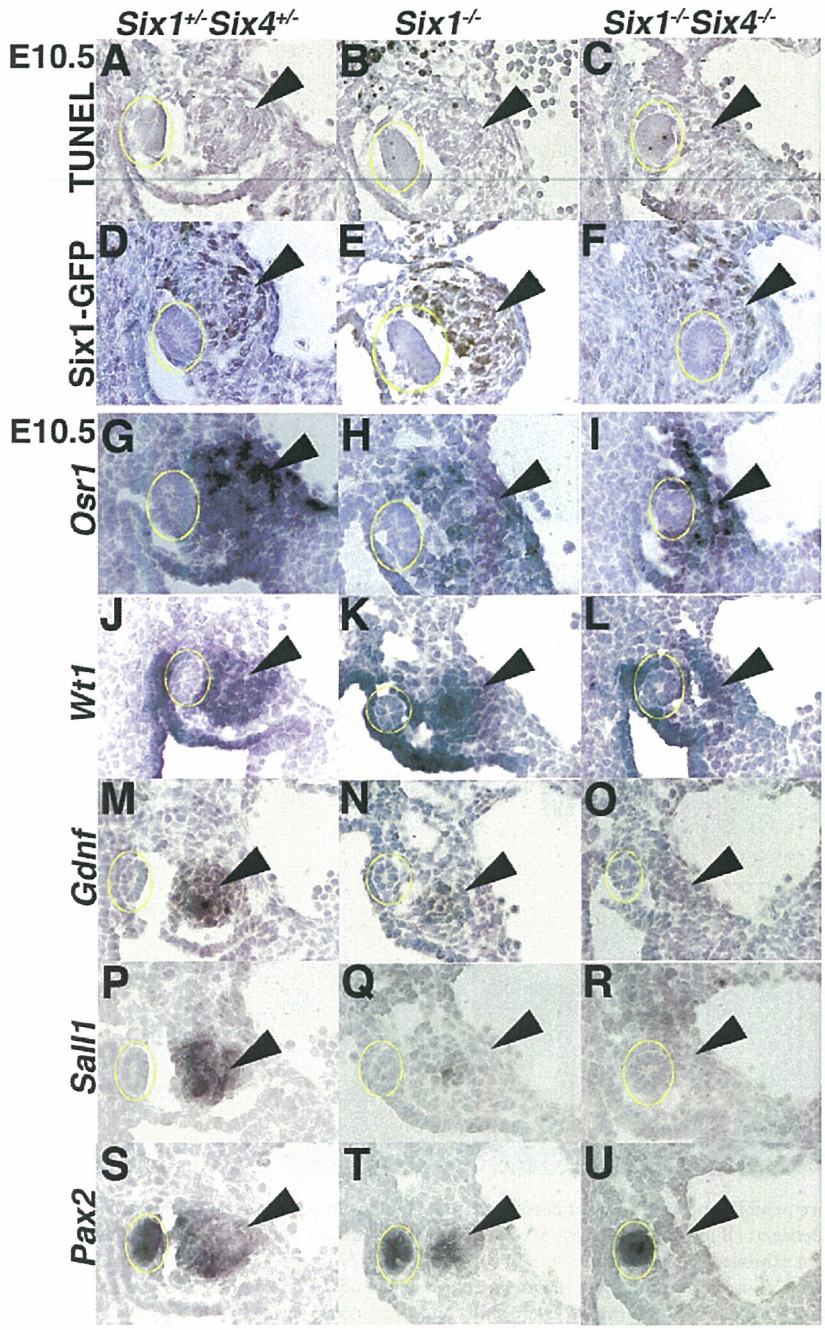

Fig. 3. *Pax2*, *Sall1*, and *Gdnf* expression is absent in the *Six1*/*Six4*-deficient metanephric mesenchyme. (A–C) TUNEL analysis of the metanephric region in the E10.5 *Six1*/*Six4*-heterozygous (A), *Six1*-deficient (B), and *Six1*/*Six4*-deficient (C) embryos. TUNEL-positive cells were not detected in the *Six1*/*Six4*-deficient metanephric mesenchyme (arrowhead). (D–F) EGFP staining in the metanephric region in the E10.5 *Six1*/*Six4*-heterozygous (D), *Six1*-deficient (E), and *Six1*/*Six4*-deficient (F) embryos. *EGFP* was knocked in the *Six1* locus. EGFP-positive cells were detected in the *Six1*/*Six4*-deficient metanephric mesenchyme. (G–I) In situ hybridization of *Osr1* in the metanephric region of the E10.5 *Six1*/*Six4*-heterozygous (G), *Six1*-deficient (H), and *Six1*/*Six4*-deficient (I) embryos. *Osr1* expression in the metanephric mesenchyme was unaffected in the *Six1*/*Six4*-deficient embryos. (J–L) *Wt1* expression in the metanephric region of the E10.5 *Six1*/*Six4*-heterozygous (J), *Six1*-deficient (K), and *Six1*/*Six4*-deficient (L) embryos. *Wt1* expression was intact in the mutant mice. (M–O) *Gdnf* expression in the metanephric region of the E10.5 *Six1*/*Six4*-heterozygous (M), *Six1*-deficient (N), and *Six1*/*Six4*-deficient (O) embryos. *Gdnf* expression was reduced in the *Six1*-deficient embryos and absent in the *Six1*/*Six4*-deficient mesenchyme. (P–R) *Sall1* expression in the metanephric region of the E10.5 *Six1*/*Six4*-heterozygous (P), *Six1*-deficient (Q), and *Six1*/*Six4*-deficient (R) embryos. *Sall1* expression was reduced in the *Six1*-deficient embryos and absent in the *Six1*/*Six4*-deficient mesenchyme. (S–U) *Pax2* expression in the metanephric region of the E10.5 *Six1*/*Six4*-heterozygous (S), *Six1*-deficient (T), and *Six1*/*Six4*-deficient (U) embryos. *Pax2* expression was reduced in the *Six1*-deficient mesenchyme and absent in the *Six1*/*Six4*-deficient mesenchyme. *Pax2* expression in the Wolffian duct remained intact in the mutant mice. The yellow circle indicates the Wolffian duct.

mesoderm (Bouchard et al., 2002). *Pax8* expression was not detected in the metanephric region at E9.5 or E10.5, while it was detected in the mesonephric region (Fig. 4A–F). However, at E10.0, *Pax8* was expressed in the metanephric mesenchyme and Wolffian duct (Fig. 4E, arrowhead) as well as in the nephrogenic cord and Wolffian duct in the mesonephric region (Fig. 4B, arrow). These results show that *Pax8* was transiently expressed in the metanephric region at E10.0.

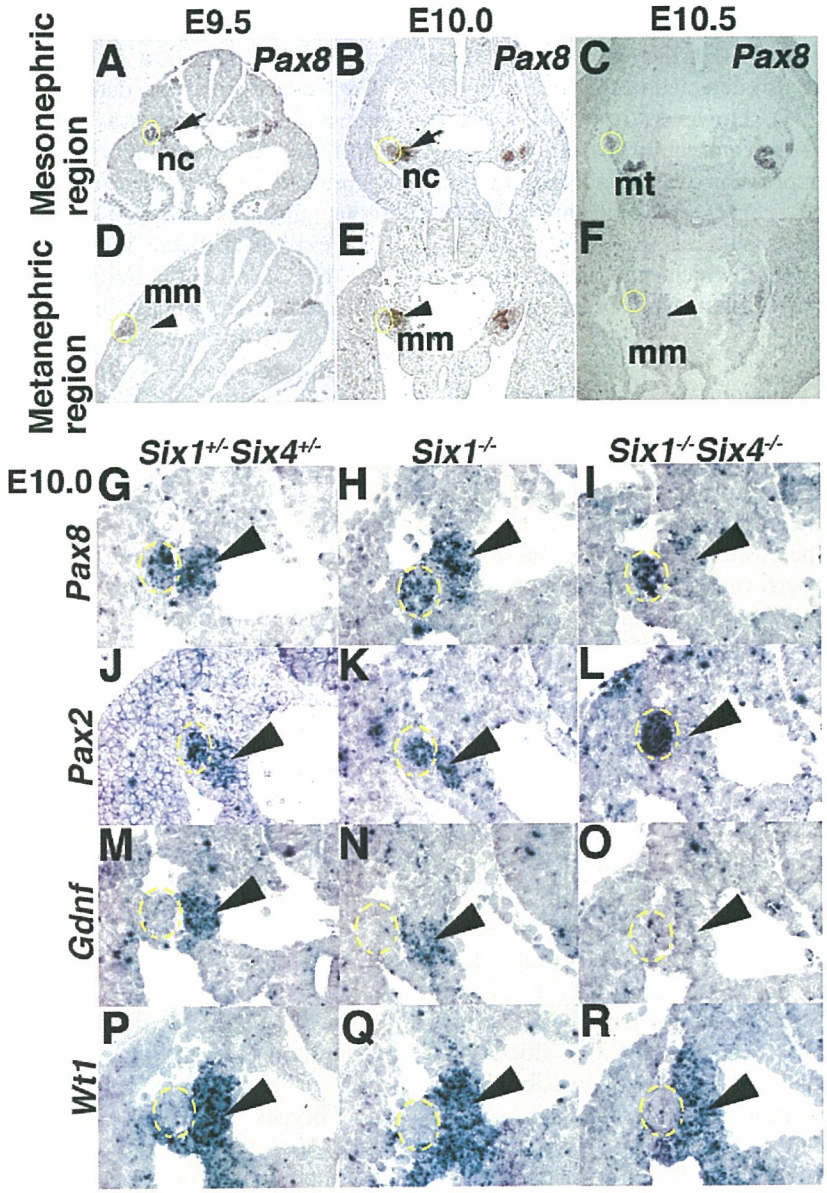

Fig. 4. *Pax8* expression is absent in the metanephric mesenchyme in *Six1*/*Six4*-deficient mice. (A–F) Transient expression of *Pax8* in the metanephric mesenchyme. *Pax8* expression in either the mesonephric (A–C) or the metanephric region (D–F) of the wild-type embryos at E9.5 (A and D), E10.0 (B and E), and E10.5 (C and F). *Pax8* expression was detected in the nephrogenic cord (arrow) and Wolffian duct (yellow circle) in the E9.5 (A) and E10.0 (B) embryos, and it was also detected in the mesonephric tubules and Wolffian duct in the E10.5 embryos (C). *Pax8* was not expressed in the metanephric mesenchyme (arrowhead) at E9.5 (D) and E10.5 (F), while it was expressed in the metanephric mesenchyme at E10.0 (E). (G–I) *Pax8* expression in the E10.0 *Six1*/*Six4*-heterozygous (G), *Six1*-deficient (H), and *Six1*/*Six4*-deficient (I) embryos. *Pax8* was expressed in the metanephric mesenchyme (arrowhead) and Wolffian duct (yellow circle) in the *Six1*/*Six4*-heterozygous (G) and *Six1*-deficient (H) embryos but not in the mesenchyme in the *Six1*/*Six4*-deficient (H) embryos. (J–L) *Pax2* expression in the E10.0 *Six1*/*Six4*-heterozygous (J), *Six1*-deficient (K), and *Six1*/*Six4*-deficient (L) embryos. *Pax2* was expressed in the metanephric mesenchyme and Wolffian duct in the *Six1*/*Six4*-heterozygous (J) and *Six1*-deficient (K) embryos but not in the mesenchyme in the *Six1*/*Six4*-deficient embryos (L). (M–O) *Gdnf* expression in the E10.0 *Six1*/*Six4*-heterozygous (M), *Six1*-deficient (N), and *Six1*/*Six4*-deficient (O) embryos. *Gdnf* expression was detected in the metanephric region in the *Six1*/*Six4*-heterozygous (M) and *Six1*-deficient (N) embryos but not in the *Six1*/*Six4*-deficient (O) embryos. (P–R) *Wt1* expression in the metanephric region of the E10.0 *Six1*/*Six4*-heterozygous (P), *Six1*-deficient (Q), and *Six1*/*Six4*-deficient (R) embryos. *Wt1* expression was maintained in the mutant mice (nc, nephrogenic cord; mt, mesonephric tubules; mm, metanephric mesenchyme).

Next, we examined *Pax8* expression in the mutant embryos at E10.0. Similar to *Pax8* expression in the wild type, it was expressed in the Wolffian duct and metanephric mesenchyme in the *Six1/Six4*-heterozygous and *Six1*-deficient embryos (Fig. 4G and H). In contrast, *Pax8* expression was absent in the mesenchyme but not in the Wolffian duct in the *Six1/Six4*-deficient embryos (Fig. 4I). Similar to the *Pax2* and *Gdnf* expression detected in the embryos examined at E10.0, the expression of these genes, although low, was also detected in the *Six1*-deficient embryos (Fig. 4K and N). However, it was completely absent in the *Six1/Six4*-deficient embryos (Fig. 4L and O). In contrast, *Wt1* expression was unaffected in both the *Six*-deficient and *Six1/Six4*-deficient embryos (Fig. 4P–R). These results suggest that *Six1* and *Six4* regulate *Pax8* as well as *Pax2*, which may possibly explain the exacerbated metanephric phenotypes of the *Six1/Six4*-deficient embryos.

2.5. *Six1* deficiency alone causes defects in the caudal mesonephric tubules

Pax2 and *Pax8* are known to be expressed in the mesonephric tubules of mouse embryos (Bouchard et al., 2002; Carroll et al., 2005). Therefore, we examined mesonephric-tubule formation by performing HE staining of sagittal sections of the E10.5 embryos. Mesonephric tubules were histologically detected in the *Six1/Six4*-heterozygous embryos (Fig. 5A). In contrast, they were not detected in the *Six1*- and *Six1/Six4*-deficient embryos (Fig. 5B and C). To confirm these findings, we performed whole-mount in situ hybridization to detect *Lim1*, which is expressed in the mesonephric tubules and Wolffian duct (Fujii et al., 1994). Mesonephric tubules and the Wolffian duct were detected in the *Six1/Six4*-heterozygous embryos (Fig. 5D). In contrast, caudal mesonephric tubules (black arrow), which are formed in the nephrogenic cord on induction by the Wolffian duct, could not be detected in the *Six1*- and *Six1/Six4*-deficient embryos (Fig. 5E and F); however, cranial tubules (white arrowhead), which develop as an outgrowth from the Wolffian duct, were detected in these embryos. To eliminate the possibility that mesonephric-tubule formation is merely delayed, we also examined the embryos at E11.5. Although mesonephric tubules were detected in the *Six1/Six4*-heterozygous embryos (Fig. 5G), only few tubules were detected in the *Six1*- and *Six1/Six4*-deficient embryos (Fig. 5H and I). To confirm these results, we performed staining for E-cadherin, which is expressed in the mesonephric tubules and Wolffian duct. Mesonephric tubules were detected along the Wolffian duct in the *Six1/Six4*-heterozygous embryos (Fig. 5J). In contrast, caudal mesonephric tubules (black arrow) were not formed in the *Six1*- and *Six1/Six4*-deficient embryos, while cranial mesonephric tubules (white arrowhead), which are derived from the Wolffian duct, were present (Fig. 5K and L). These results indicate that *Six1* deficiency alone causes mesonephric-tubule defects and that the *Six1/Six4*-deficient embryos exhibit a phenotype comparable to that of the *Six1*-deficient embryos.

2.6. *Pax2* expression is absent in the nephrogenic cord in *Six1*-deficient mice

Next, we investigated the expression of the genes essential for mesonephric-tubule formation by performing in situ hybridization in the nephrogenic cord at E9.5. *Osr1* expression was detected in the *Six1/Six4*-heterozygous embryos and was maintained in the *Six1*- and *Six1/Six4*-deficient embryos (Fig. 6A–C). *Wt1* was also expressed in both the mutants and *Six1/Six4*-heterozygous embryos (Fig. 6D–F). In contrast, *Pax2*, which was expressed in the Wolffian duct and nephrogenic cord in the *Six1/Six4*-heterozygous embryos, could not be detected in the nephrogenic cord of the *Six1*- and *Six1/Six4*-deficient embryos. However *Pax2* expression was maintained in the Wolffian duct (Fig. 6G–I). *Pax8* was also detected in the Wolffian duct and nephrogenic cord in the *Six1/Six4*-heterozygous embryos and the *Six1*-deficient embryos retained *Pax8* expression in the nephrogenic cord, while the *Six1/Six4*-deficient cords lacked the expression (Fig. 6J–L). These results suggest that *Pax2* and *Pax8* are regulated by *Six1* and *Six4* in the nephrogenic cord, similar to the metanephric mesenchyme. However, *Six1*-mediated *Pax2* activation but not *Six1/Six4*-dependent *Pax8* upregulation may play a central role in mesonephric tubule formation, unlike the situation in the metanephros. This is because *Six1* deficiency alone is sufficient to affect *Pax2* expression and cause mesonephric-tubule defects. *Wnt9b*, which was expressed in the Wolffian duct, was unaffected in both mutant embryos (Fig. 6M–O); this indicates that the kidney phenotypes could not be accounted for by *Wnt9b* deficiency in the Wolffian duct.

3. Discussion

In this paper, we demonstrate that *Six1* and *Six4* have redundant roles in kidney development, and that inactivation of both genes leads to more severe metanephric phenotypes than those of *Six1*-deficient mice. In the *Six1/Six4*-deficient mice, a distinct cell cluster is absent in the metanephric mesenchyme, and the ureteric bud is not formed. However, both these components are present in the *Six1*-deficient mice, although they are impaired. In contrast, mesonephric tubules are absent in both the *Six1*- and *Six1/Six*4-deficient mice, suggesting that *Six4* plays a minor role in mesonephros formation.

The expression of *Pax2* and *Gdnf* is partially lowered in the *Six1*-deficient mice and absent in the *Six1/Six4*-deficient mice. In contrast, *Pax8* expression is absent only in the double mutant mice. These results indicate that *Pax2* and *Gdnf* are regulated mainly by *Six1* and partially by *Six4*, while *Pax8* expression is maintained when either *Six1* or *Six4* is present. *Sall1* is almost absent in the

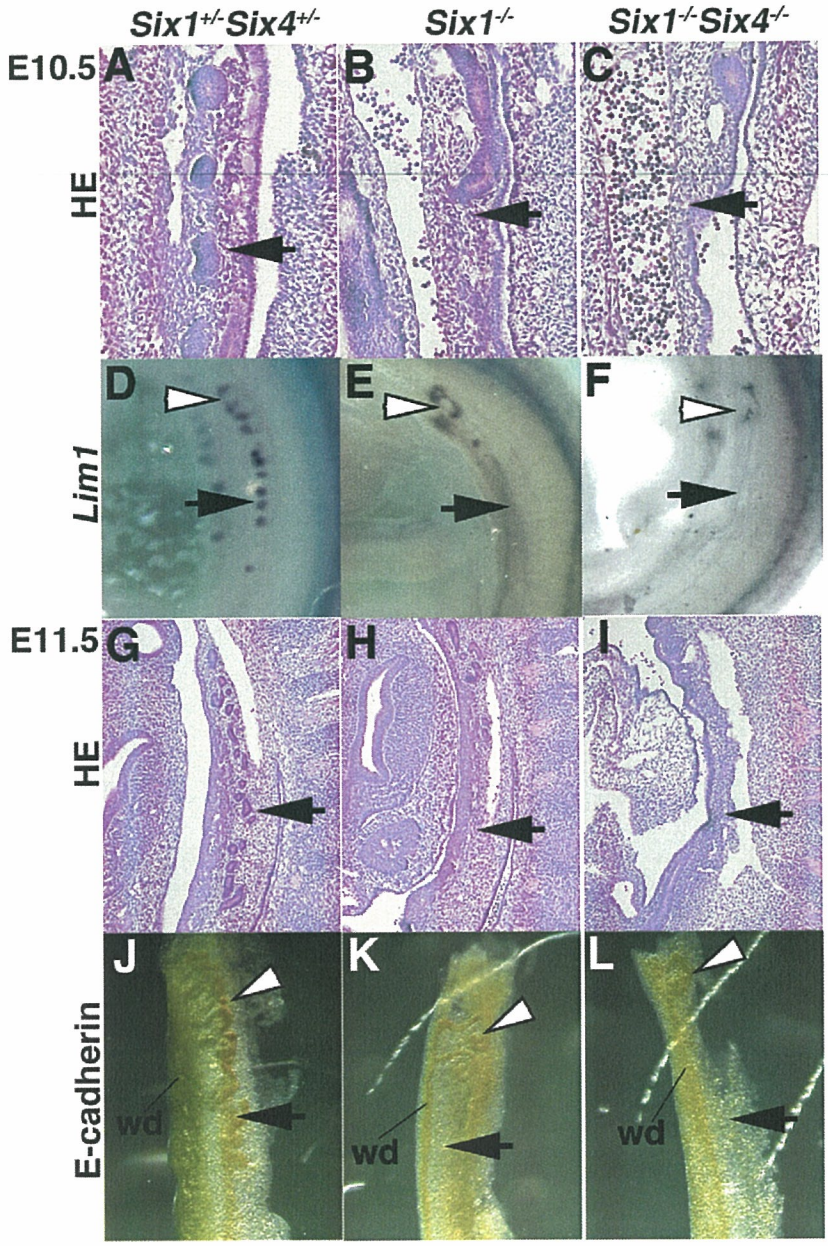

Fig. 5. Caudal mesonephric tubules are not formed in the *Six1*- and *Six1/Six4*-deficient embryos. (A–C) HE staining of the sagittal sections of the mesonephric region of the E10.5 *Six1/Six4*-heterozygous (A), *Six1*-deficient (B), and *Six1/Six4*-deficient (C) embryos. Several mesonephric tubules (arrow) were observed in the *Six1/Six4*-heterozygous embryos (A) but they were fewer in the *Six1*- (B) and *Six1/Six4*-deficient embryos (C). (D–F) Whole-mount in situ hybridization of *Lim1* in the mesonephros of the E10.5 *Six1/Six4*-heterozygous (D), *Six1*-deficient (E), and *Six1/Six4*-deficient (F) embryos. *Lim1*-positive mesonephric tubules were observed lined in the craniocaudal direction in the *Six1/Six4*-heterozygous embryos (D), while *Lim1*-positive caudal mesonephric tubules (black arrow) were not observed in the *Six1*- (E) and *Six1/Six4*-deficient (F) embryos. (G–I) HE staining of the sagittal sections of the mesonephric region of the E11.5 *Six1/Six4*-heterozygous (G), *Six1*-deficient (H), and *Six1/Six4*-deficient (I) embryos. Many mesonephric tubules were observed in the *Six1/Six4*-heterozygous embryos (G), while few were observed in the *Six1*- (H) and *Six1/Six4*-deficient embryos (I). (J–L) Whole-mount immunostaining of E-cadherin, which is expressed in the mesonephric tubules and the Wolffian duct, in the mesonephros of the E11.5 *Six1/Six4*-heterozygous (J), *Six1*-deficient (K), and *Six1/Six4*-deficient (L) embryos. Many mesonephric tubules were observed lined in the craniocaudal direction in the *Six1/Six4*-heterozygous embryos (J), while caudal mesonephric tubules were not observed in the *Six1*- (K) and *Six1/Six4*-deficient embryos (L). The white arrowhead indicates the cranial mesonephric tubules (wd, Wolffian duct).

Six1-deficient mice, and *Six4* may play a minimal role in the expression of this gene. This differential regulation could result either from the difference in the amount of the two corresponding gene products in the tissue or from the binding specificity of the DNA-binding domains to the target sequences. Previously, we reported that the promoter region of the *sodium-potassium-chloride cotransporter 1*(*Scl1 2a2*) gene is a common target of Six1 and Six4,

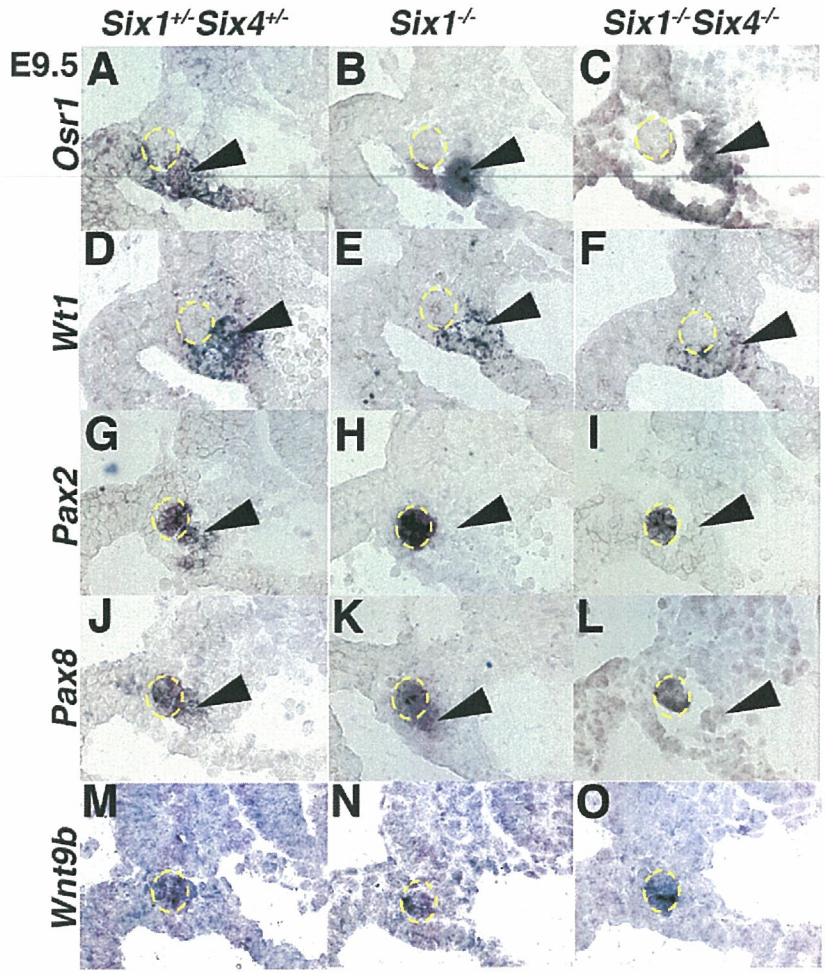

Fig. 6. *Pax2* expression is absent in the nephrogenic cord in *Six1*-deficient embryos. (A–C) In situ hybridization of *Osr1* in the mesonephric region of the E9.5 *Six1*/*Six4*-heterozygous (A), *Six1*-deficient (B), and *Six1*/*Six4*-deficient (C) embryos. *Osr1* expression in the nephrogenic cord (arrow) remained intact in the *Six1*- (B) and *Six1*/*Six4*-deficient embryos (C). (D–F) *Wt1* expression in the mesonephric region of the *Six1*/*Six4*-heterozygous (D), *Six1*-deficient (E), and *Six1*/*Six4*-deficient (F) embryos at E9.5. *Wt1* expression in the nephrogenic cord (D) remained intact in the *Six1*- (E) and *Six1*/*Six4*-deficient (F) embryos. (G–I) *Pax2* expression in the mesonephric region of the E9.5 *Six1*/*Six4*-heterozygous (G), *Six1*-deficient (H), and *Six1*/*Six4*-deficient (I) embryos. *Pax2* expression in the nephrogenic cord was absent in the *Six1*- (H) and *Six1*/*Six4*-deficient (I) embryos. (J–L) *Pax8* expression in the mesonephric region of the *Six1*/*Six4*-heterozygous (J), *Six1*-deficient (K), and *Six1*/*Six4*-deficient (L) embryos at E9.5. *Pax8* expression in the nephrogenic cord is absent in the *Six1*/*Six4*-deficient embryos (L) but not in the *Six1*-deficient embryos (K). (M–O) *Wnt9b* expression in the mesonephric region of the E9.5 *Six1*/*Six4*-heterozygous (M), *Six1*-deficient (N), and *Six1*/*Six4*-deficient (O) embryos. *Wnt9b* expression in the Wolffian duct (yellow circle) was unaffected in the mutant embryos.

and that this region contains multiple Six1-binding sites and one common binding site for Six1 and Six4 (Ando et al., 2005). A similar mechanism may also underlie the differential regulation of common target genes during kidney development.

The *Six* gene family has a consensus binding site, and Six1 is reported to bind to the first intron of *Gdnf* (Li et al., 2003) – a key attractant for ureteric budding. Further, Pax2 binds to the 5'-untranslated region of *Gdnf* exon 1 (Brophy et al., 2001). Six2 also binds to the *Gdnf* promoter region and activates *Gdnf* expression (Brodbeck et al., 2004). However, *Six2* expression is absent in *Six1*-deficient mouse embryos (data not shown; Xu et al., 2003). These results are consistent with the findings that both the *Six1*- and *Pax2*-deficient mice show incomplete ureteric-bud invasion into the mesenchyme (Brophy et al., 2001; Li et al., 2003). Though the mechanism underlying the direct binding of Six4 to the promoters remains to be elucidated, *Six1* and *Six4* may regulate *Gdnf* expression in two ways – directly or indirectly. The former is executed by binding to the *Gdnf* promoter and the latter, via *Pax2* and *Pax8*. Thus, inactivation of *Six1* and *Six4* should lead to a complete absence of *Gdnf*, a critical factor for ureteric bud formation. This reveals a redundancy in the *Six-Pax-Gdnf* pathway. *Eya1* is a cofactor for *Six1*-dependent transcriptional activation, and the loss of *Eya1* in mice leads to a metanephric phenotype similar to that of *Six1*/*Six4*-deficient mice and more severe than that of

the *Six1*-deficient mice; *Pax2* and *Gdnf* expression is completely absent in this phenotype (Xu et al., 1999; Nica et al., 2006). Hence, it is possible that both Six1 and Six4 cooperate with Eya1, thus regulating *Pax2*/*Pax8* and *Gdnf* expression.

Mesonephric tubules were absent in both the *Six1*- and *Six1*/*Six4*-deficient mice. Although several researchers have reported metanephric abnormalities in *Six1*-null mice (Laclef et al., 2003a; Li et al., 2003; Xu et al., 2003), this is the first report of mesonephric phenotypes in these mice. *Pax2* was absent in the *Six1*- and *Six1*/*Six4*-deficient mice, while *Pax8* remained undetected only in the *Six1*/*Six4*-deficient mice. This resembled a cascade similar to that occurring during metanephros formation. However, the absence of *Six4* did not exacerbate the defects observed in *Six1* deficiency; this suggests that a reduction in *Pax8* expression does not contribute to the lack of mesonephric tubules and that *Pax2* expression may play a major role in this process. Consistent with this finding, Torres et al. (1995) reported that mesonephric-tubule formation is impaired in *Pax2*-deficient mice. Thus, *Six1*-dependent *Pax2* activation in the nephrogenic cord (a mesenchymal tissue) could be a prerequisite for mesonephric-tubule formation, which involves a mesenchymal-to-epithelial transition induced by signals, including Wnt9b from the Wolffian duct (Carroll et al., 2005).

Pax2 and *Pax8* are expressed in the intermediate mesoderm, and these two genes must play a major role in directing the intermediate mesoderm toward nephrogenic lineage because mice deficient in both these genes lack Wolffian-duct formation (Bouchard et al., 2002). In contrast, in *Six1*/*Six4*-null mice, direction toward kidney lineage occurs, although *Pax2* and *Pax8* expression is abolished. This apparent inconsistency can be explained by studying the expression domains of these genes. *Six1* and *Six4* are expressed in the nephrogenic mesenchyme (nephrogenic cord and metanephric mesenchyme) but not in the Wolffian duct, while *Pax2* and *Pax8* are expressed in each of these intermediate mesoderm-derived components. In the absence of *Six1* and *Six4*, *Pax2* and *Pax8* expression is reduced in the nephrogenic mesenchyme but not in the Wolffian duct (Fig. 6T, L). Therefore, *Six1*/*Six4*-null mice tend to exhibit mesenchyme-specific lowering of *Pax2* and *Pax8* expression; thus, they exhibit a milder phenotype than conventional *Pax2*/*Pax8*-deficient mice. In the mesenchyme, *Six1* and *Six4* are located upstream of *Pax2* and *Pax8*, as mentioned in this paper. This cascade does not exist in the Wolffian duct. Instead, *Pax2*/*Pax8*-dependent *Gata3* activation is reported to regulate migration of the Wolffian duct toward the cloaca. In *Gata3*-null mice, mesenchymal migration is maintained, and *Pax2* expression in the mesenchyme (and possibly the expression of its upstream regulators *Six1* and *Six4*) is not affected (Grote et al., 2006). Thus, the *Six-Pax* cascade in the mesenchyme and the *Pax-Gata3* pathway in the Wolffian duct may operate independently.

Our data place *Six1* and *Six4* upstream of *Pax2* and *Pax8* in the mesenchymal tissues in both the metanephros and mesonephros. In addition, our data further elaborates on the findings of Xu et al., revealing that *Six1* is located upstream of *Pax2* during metanephric development (Xu et al., 2003). This *Six-Pax* cascade is distinct from the situation in *Drosophila*, in which *sine oculis* (*Six* homolog) is located downstream of *eyeless* (*Pax* homolog). However, the *Six-Pax* cascade is conserved during mammalian muscle development, where *Six1* and *Six4* are located upstream of *Pax3* and *Met* and regulate myogenic migration in somites (Grifone et al., 2005). Then how are *Six1* and *Six4* regulated in the nephrogenic mesenchyme? A recent study predicted the TCF4- and Gli-binding sites in the promoters of *Six1* and *Six4* by using computational methods, suggesting that Wnt and hedgehog may regulate the *Six* genes (Hallikas et al., 2006). In fact, *Six1* expression in the limb buds is reduced in *Shh* mutants (Bonnin et al., 2005). In the metanephros, *Shh* deficiency leads to a reduction in *Pax2* and *Sall1* genes downstream of *Six1* (Hu et al., 2006). Thus, an analysis using mutant mice that lack the candidate soluble factors may further reveal the details of the *Six-Pax* cascade that controls kidney formation.

Finally, *Six1* mutation is reported to be associated with the branchio-oto-renal syndrome, which leads to kidney or urinary tract malformation (Ruf et al., 2004). In addition, a deletion at 14q22–23 that overlaps the *SIX1* and *SIX4* loci causes multiple abnormalities, including renal hypoplasia (Bennett et al., 1991). Thus, an analysis of *Six1*/*Six4*-deficient mice may be useful for elucidating the mechanism underlying these diseases.

4. Experimental procedures

4.1. Generating mutant mice and confirming their genotype

The procedure for generating *Six1*- and *Six1*/*Six4*-deficient mice has been previously described (Ozaki et al., 2004; Konishi et al., 2006). *Six1*/*Six4*-deficient mice carry a targeted in-frame fusion of the *EGFP* gene into the first coding exon of the *Six1* gene and that of the *LacZ* gene into the first coding exon of the *Six4* gene. Mice and embryos from subsequent generations were genotyped by PCR. The *Six1* mutant allele was detected using the primers WtmSix1F (5′-GCGCCCGGGCC CGTGCGCCCC-3′) and KOmSix1R (5′-TGCCCCAGGATGTTGCC GTCC-3′), and the wild-type allele was detected using the primers WtmSix1F and WtmSix1R (5′-GCTTTCAGCCACAGCTGCTGC-3′). The length of the PCR products was 323 and 470 bp in the wild-type and mutant alleles, respectively. The *Six4* mutant allele was detected using the primers WtmSix4F (5′-ACATCAAGCAGGAGAATGGGATGG-3′) and KOmSix4R (5′-CCGTAATGGGATAGGTTACGTTGG-3′), and the wild-type allele was detected using the primers WtmSix4F and WtmSix4R (5′-AGAAGTTCCGAGTGGAGTTGTACC-3′). The length of the PCR products was 212 and 445 bp in the wild-type and mutant alleles, respectively.

4.2. Histological examination

The embryos were fixed in 10% formalin in phosphate-buffered saline (PBS). The dehydrated specimens were embedded in paraffin wax and subsequently cut into 6-μm thick serial sections, de-waxed, and then stained with HE.

4.3. RNA in situ hybridization

The embryos were fixed by incubating them at 4 °C overnight in 10% formalin in PBS. After washing the samples with PBS containing 30% sucrose, they were embedded in OCT compound (Tissue-Tek), frozen, and cut into 10-μm thick serial cryosections. In situ hybridization was performed using digoxigenin-labeled antisense riboprobes, as described previously (Nishinakamura et al., 2001). We used the TSA-amplification kit (PerkinElmer) when required. For whole-mount in situ hybridization, the dissected urogenital tissues were fixed by incubating them at 4 °C overnight in 10% formalin in PBS; they were then dehydrated using a methanol series. Prior to hybridization, the specimens were treated with 20 μg/ml proteinase K (Roche) for 15 min, followed by hybridization with a labeled RNA probe at 68 °C overnight (1 μg/ml). Post hybridization, the specimens were washed twice with 0.1% CHAPS/2 × SSC at 68 °C for 20 min each time; they were then incubated with RNase A (20 μg/ml; 2 × SSC; 37 °C; 30 min) and washed twice with 0.1% CHAPS/0.2 × SSC at 68 °C for 20 min each time. Further, the specimens were blocked with PBS containing 10% sheep serum and 0.1% Triton X-100 and incubated with alkaline phosphatase-conjugated anti-digoxigenin antibody (1:2000 in PBT, Roche) overnight at 4 °C. The samples were developed by using NBT and BCIP. We used the cDNA of the following genes as in situ hybridization probes: *Pax2*, *WT1*, *Sall1*, *Gdnf* (Nishinakamura et al., 2001), and *Wnt9b* (a kind gift from A.P. McMahon). The cDNA for other probes was isolated by PCR, subcloned into pBluescript KS(-), and sequenced. None of the sense probes produced signals.

4.4. Whole-mount immunohistochemistry

The dissected urogenital tissues were fixed in 10% formalin in PBS and treated with 0.3% H_2O_2 in methanol for 60 min. After washing the specimens with PBT (PBS with 1% Triton X-100), they were incubated at 4 °C for 2 h in a blocking solution containing 1% skim milk and 1% normal goat serum in PBT. The specimens were then incubated at 4 °C for 16 h with a mouse primary antibody against E-cadherin (1:1000 in PBT, Becton Dickinson). They were then washed with PBT and incubated at 4 °C for 16 h with a peroxidase-conjugated goat secondary antibody against rabbit IgG (1:500 in PBT, KPL). The samples were developed by incubating them for 30 min with 0.2 mg/ml DAB and 0.01% H_2O_2 in PBS. The specimens were fixed in 10% formalin in PBS and cleaned with 75% glycerol for microscopic observation.

4.5. TUNEL analysis

The cryosections were fixed in 1% paraformaldehyde in PBS and permeabilized with 30% acetic acid in ethanol for 5 min at −30 °C. TUNEL analysis was performed by using the Apoptag In Situ Cell Death Detection Kit (Chemicon). In brief, fragmented DNA in apoptotic cells was end-labeled with digoxigenin, and the labeled DNA was detected using a peroxidase-conjugated anti-digoxigenin antibody, stained using a metal-enhanced DAB kit (Pierce), and counterstained with hematoxylin.

Acknowledgements

The authors thank S.S. Tanaka, C. Kobayashi, T. Inenaga, and M. Takasato for their critical suggestions and A.P. McMahoon for providing the *Wnt9b* probe. This work was supported in part by the Ministry of Education, Culture, Sports, Science and Technology and the Ministry of Health, Labor and Welfare of Japan and the Research Fellowships of the Japan Society for the promotion of Science for Young Scientists.

References

Ando, Z., Sato, S., Ikeda, K., Kawakami, K., 2005. *Slc12a2* is a direct target of two closely related homeobox proteins, Six1 and Six4. FEBS J. 272, 3026–3041.

Bennett, C.P., Betts, D.R., Seller, M.J., 1991. Deletion 14q (q22q23) associated with anophthalmia, absent pituitary, and other abnormalities. J. Med. Genet. 28, 280–281.

Bonnin, M.A., Laclef, C., Blaise, R., Eloy-Trinquet, S., Relaix, F., Maire, P., Duprez, D., 2005. *Six1* is not involved in limb tendon development, but is expressed in limb connective tissue under Shh regulation. Mech. Dev. 122, 573–585.

Bouchard, M., Souabni, A., Mandler, M., Neubuser, A., Busslinger, M., 2002. Nephric lineage specification by Pax2 and Pax8. Genes Dev. 16, 2958–2970.

Brodbeck, S., Besenbeck, B., Englert, C., 2004. The transcription factor Six2 activates expression of the *Gdnf* gene as well as its own promoter. Mech. Dev. 121, 1211–1222.

Brophy, P.D., Ostrom, L., Lang, K.M., Dressler, G.R., 2001. Regulation of ureteric bud outgrowth by Pax2-dependent activation of the glial derived neurotrophic factor gene. Development 128, 4747–4756.

Cacalano, G., Farinas, I., Wang, L.C., Hagler, K., Forgie, A., Moore, M., Armanini, M., Phillips, H., Ryan, A.M., Reichardt, L.F., Hynes, M., Davies, A., Rosenthal, A., 1998. GFRalpha1 is an essential receptor component for GDNF in the developing nervous system and kidney. Neuron 21, 53–62.

Carl, M., Loosli, F., Wittbrodt, J., 2002. *Six3* inactivation reveals its essential role for the formation and patterning of the vertebrate eye. Development 129, 4057–4063.

Carroll, T.J., Park, J.S., Hayashi, S., Majumdar, A., McMahon, A.P., 2005. Wnt9b plays a central role in the regulation of mesenchymal to epithelial transitions underlying organogenesis of the mammalian urogenital system. Dev. Cell 9, 283–292.

Durbec, P., Marcos-Gutierrez, C.V., Kilkenny, C., Grigoriou, M., Wartiowaara, K., Suvanto, P., Smith, D., Ponder, B., Costantini, F., Saarma, M., Sariola, H., Pachnis, V., 1996. GDNF signaling through the Ret receptor tyrosine kinase. Nature 381, 789–793.

Enomoto, H., Araki, T., Jackman, A., Heuckeroth, R.O., Snider, W.D., Johnson Jr., E.M., Milbrandt, J., 1998. GFR alpha1-deficient mice have deficits in the enteric nervous system and kidneys. Neuron 21, 317–324.

Fujii, T., Pichel, J.G., Taira, M., Toyama, R., Dawid, I.B., Westphal, H., 1994. Expression patterns of the murine LIM class homeobox gene *lim1* in the developing brain and excretory system. Dev. Dyn. 199, 73–83.

Grifone, R., Demignon, J., Houbron, C., Souil, E., Niro, C., Seller, M.J., Hamard, G., Maire, P., 2005. Six1 and Six4 homeoproteins are required for Pax3 and Mrf expression during myogenesis in the mouse embryo. Development 132, 2235–2249.

Grobstein, C., 1953. Morphogenetic interaction between embryonic mouse tissues separated by a membrane filter. Nature 172, 869–870.

Grote, D., Souabni, A., Busslinger, M., Bouchard, M., 2006. Pax 2/8-regulated Gata3 expression is necessary for morphogenesis and guidance of the nephric duct in the developing kidney. Development 133, 53–61.

Hallikas, O., Palin, K., Sinjushina, N., Rautiainen, R., Partanen, J., Ukkonen, E., Taipale, J., 2006. Genome-wide prediction of mammalian enhancers based on analysis of transcription-factor binding affinity. Cell 124, 47–59.

Himeda, C.L., Ranish, J.A., Angello, J.C., Maire, P., Aebersold, R., Hauschka, S.D., 2004. Quantitative proteomic identification of six4 as the trex-binding factor in the muscle creatine kinase enhancer. Mol. Cell. Biol. 24, 2132–2143.

Hu, M.C., Mo, R., Bhella, S., Wilson, C.W., Chuang, P.T., Hui, C.C., Rosenblum, N.D., 2006. GLI3-dependent transcriptional repression of *Gli1*, *Gli2* and kidney patterning genes disrupts renal morphogenesis. Development 133, 569–578.

James, R.G., Schultheiss, T.M., 2003. Patterning of the avian intermediate mesoderm by lateral plate and axial tissues. Dev. Biol. 253, 109–124.

James, R.G., Schultheiss, T.M., 2005. Bmp signaling promotes intermediate mesoderm gene expression in a dose-dependent, cell-autonomous and translation-dependent manner. Dev. Biol. 288, 113–125.

James, R.G., Kamei, C.N., Wang, Q., Jiang, R., Schultheiss, T.M., 2006. Odd-skipped related 1 is required for development of the metanephric kidney and regulates formation and differentiation of kidney precursor cells. Development 133, 2995–3004.

Kawakami, K., Sato, S., Ozaki, H., Ikeda, K., 2000. *Six* family genes – structure and function as transcription factors and their roles in development. Bioessays 22, 616–626.

Kobayashi, A., Kwan, K.M., Carroll, T.J., McMahon, A.P., Mendelsohn, C.L., Behringer, R.R., 2005. Distinct and sequential tissue-specific activities of the LIM-class homeobox gene *Lim1* for tubular morphogenesis during kidney development. Development 132, 2809–2823.

Kobayashi, M., Toyama, R., Takeda, H., Dawid, I.B., Kawakami, K., 1998. Overexpression of the forebrain-specific homeobox gene six3 induces rostral forebrain enlargement in zebrafish. Development 125, 2973–2982.

Konishi, Y., Ikeda, K., Iwakura, Y., Kawakami, K., 2006. *Six1* and *Six4* promote survival of sensory neurons during early trigeminal gangliogenesis. Brain Res. 1116, 93–102.

Kreidberg, J.A., Sariola, H., Loring, J.M., Maeda, M., Pelletier, J., Housman, D., Jaenisch, R., 1993. WT-1 is required for early kidney development. Cell 74, 679–691.

Laclef, C., Hamard, G., Demignon, J., Souil, E., Houbron, C., Maire, P., 2003a. Altered myogenesis in *Six1*-deficient mice. Development 130, 2239–2252.

Laclef, C., Souil, E., Demignon, J., Maire, P., 2003b. Thymus, kidney and craniofacial abnormalities in *Six 1* deficient mice. Mech. Dev. 120, 669–679.

Lagutin, O.V., Zhu, C.C., Kobayashi, D., Topczewski, J., Shimamura, K., Puelles, L., Russell, H.R., McKinnon, P.J., Solnica-Krezel, L., Oliver, G., 2003. Six3 repression of Wnt signaling in the anterior neuroectoderm is essential for vertebrate forebrain development. Genes Dev. 17, 368–379.

Li, X., Oghi, K.A., Zhang, J., Krones, A., Bush, K.T., Glass, C.K., Nigam, S.K., Aggarwal, A.K., Maas, R., Rose, D.W., Rosenfeld, M.G., 2003. Eya protein phosphatase activity regulates Six1-Dach-Eya transcriptional effects in mammalian organogenesis. Nature 426, 254–274.

Loosli, F., Winkler, S., Wittbrodt, J., 1999. *Six3* overexpression initiates the formation of ectopic retina. Genes Dev. 13, 649–654.

Lopez-Rios, J., Tessmar, K., Loosli, F., Wittbrodt, J., Bovolenta, P., 2003. Six3 and Six6 activity is modulated by members of the groucho family. Development 130, 185–195.

Mauch, T.J., Yang, G., Wright, M., Smith, D., Schoenwolf, G.C., 2000. Signals from trunk paraxial mesoderm induce pronephros formation in chick intermediate mesoderm. Dev. Biol. 220, 62–75.

Moore, M.W., Klein, R.D., Farinas, I., Sauer, H., Armanini, M., Phillips, H., Reichardt, L.F., Ryan, A.M., Carver-Moore, K., Rosenthal, A., 1996. Renal and neuronal abnormalities in mice lacking *GDNF*. Nature 382, 76–79.

Nica, G., Herzog, W., Sonntag, C., Nowak, M., Schwarz, H., Zapata, A.G., Hammerschmidt, M., 2006. Eya1 is required for lineage-specific differentiation, but not for cell survival in the zebrafish adenohypophysis. Dev. Biol. 292, 189–204.

Nishinakamura, R., Matsumoto, Y., Nakao, K., Nakamura, K., Sato, A., Copeland, N.G., Gilbert, D.J., Jenkins, N.A., Scully, S., Lacey, D.L., Katsuki, M., Asashima, M., Yokota, T., 2001. Murine homolog of *SALL1* is essential for ureteric bud invasion in kidney development. Development 128, 3105–3115.

Obara-Ishihara, T., Kuhlman, J., Niswander, L., Herzlinger, D., 1999. The surface ectoderm is essential for nephric duct formation in intermediate mesoderm. Development 126, 1103–1108.

Oliver, G., Wehr, R., Jenkins, N.A., Copeland, N.G., Cheyette, B.N., Hartenstein, V., Zipursky, S.L., Gruss, P., 1995. Homeobox genes and connective tissue patterning. Development 121, 693–705.

Ozaki, H., Watanabe, Y., Takahashi, K., Kitamura, K., Tanaka, A., Urase, K., Momoi, T., Sudo, K., Sakagami, J., Asano, M., Iwakura, Y., Kawakami, K., 2001. *Six4*, a putative *myogenin* gene regulator, is not essential for mouse embryonal development. Mol. Cell. Biol. 21, 3343–3350.

Ozaki, H., Nakamura, K., Funahashi, J., Ikeda, K., Yamada, G., Tokano, H., Okamura, H.O., Kitamura, K., Muto, S., Kotaki, H., Sudo, K., Horai, R., Iwakura, Y., Kawakami, K., 2004. Six1 controls patterning of the mouse otic vesicle. Development 131, 551–562.

Pichel, J.G., Shen, L., Sheng, H.Z., Granholm, A.C., Drago, J., Grinberg, A., Lee, E.J., Huang, S.P., Saarma, M., Hoffer, B.J., Sariola, H., Westphal, H., 1996. Defects in enteric innervation and kidney development in mice lacking *GDNF*. Nature 382, 73–76.

Ruf, R.G., Xu, P.X., Silvius, D., Otto, E.A., Beekmann, F., Muerb, U.T., Kumar, S., Neuhaus, T.J., Kemper, M.J., Raymond Jr., R.M., Brophy, P.D., Berkman, J., Gattas, M., Hyland, V., Ruf, E.M., Schwartz, C., Chang, E.H., Smith, R.J., Stratakis, C.A., Weil, D., Petit, C., Hildebrandt, F., 2004. SIX1 mutations cause branchio-oto-renal syndrome by disruption of EYA1-SIX1-DNA complexes. Proc. Natl. Acad. Sci. USA 101, 8090–8095.

Sainio, K., Hellstedt, P., Kreidberg, J.A., Saxen, L., Sariola, H., 1997a. Differential regulation of two sets of mesonephric tubules by WT-1. Development 124, 1293–1299.

Sainio, K., Suvanto, P., Davies, J., Wartiovaara, J., Wartiovaara, K., Saarma, M., Arumae, U., Meng, X., Lindahl, M., Pachnis, V., Sariola, H., 1997b. Glial-cell-line-derived neurotrophic factor is required for bud initiation from ureteric epithelium. Development 124, 4077–4087.

Sanchez, M.P., Silos-Santiago, I., Frisen, J., He, B., Lira, S.A., Barbacid, M., 1996. Renal agenesis and the absence of enteric neurons in mice lacking GDNF. Nature 382, 70–73.

Sariola, H., Saarma, M., 1999. GDNF and its receptors in the regulation of the ureteric branching. Int. J. Dev. Biol. 43, 413–418.

Sarkar, P.S., Appukuttan, B., Han, J., Ito, Y., Ai, C., Tsai, W., Chai, Y., Stout, J.T., Reddy, S., 2000. Heterozygous loss of *Six5* in mice is sufficient to cause ocular cataracts. Nat. Genet. 25, 110–114.

Sarkar, P.S., Paul, S., Han, J., Reddy, S., 2004. Six5 is required for spermatogenic cell survival and spermiogenesis. Hum. Mol. Genet. 13, 1421–1431.

Saxen, L., 1987. Organogenesis of the Kidney. Cambridge University Press, London.

Spitz, F., Demignon, J., Porteu, A., Kahn, A., Concordet, J.P., Daegelen, D., Maire, P., 1998. Expression of myogenin during embryogenesis is controlled by Six/sine oculis homeoproteins through a conserved MEF3 binding site. Proc. Natl. Acad. Sci. USA 95, 14220–14225.

Torres, M., Gomez-Pardo, E., Dressler, G.R., Gruss, P., 1995. Pax-2 controls multiple steps of urogenital development. Development 121, 4057–4065.

Tsang, T.E., Shawlot, W., Kinder, S.J., Kobayashi, A., Kwan, K.M., Schughart, K., Kania, A., Jessell, T.M., Behringer, R.R., Tam, P.P., 2000. Lim1 activity is required for intermediate mesoderm differentiation in the mouse embryo. Dev. Biol. 223, 77–90.

Vainio, S., Lin, Y., 2002. Coordinating early kidney development: lessons from gene targeting. Nat. Rev. Genet. 3, 533–543.

Wang, Q., Lan, Y., Cho, E.S., Maltby, K.M., Jiang, R., 2005. Odd-skipped related 1 (Odd 1) is an essential regulator of heart and urogenital development. Dev. Biol. 288, 582–594.

Xu, P.X., Adams, J., Peters, H., Brown, M.C., Heaney, S., Maas, R., 1999. *Eya1*-deficient mice lack ears and kidneys and show abnormal apoptosis of organ primordia. Nat. Genet. 23, 113–117.

Xu, P.X., Zheng, W., Huang, L., Maire, P., Laclef, C., Silvius, D., 2003. Six1 is required for the early organogenesis of mammalian kidney. Development 130, 3085–3094.

Zheng, W., Huang, L., Wei, Z.B., Silvius, D., Tang, B., Xu, P.X., 2003. The role of Six1 in mammalian auditory system development. Development 130, 3989–4000.

Zhu, C.C., Dyer, M.A., Uchikawa, M., Kondoh, H., Lagutin, O.V., Oliver, G., 2002. Six3-mediated auto repression and eye

development requires its interaction with members of the Groucho-related family of co-repressors. Development 129, 2835–2849.

Zou, D., Silvius, D., Fritzsch, B., Xu, P.X., 2004. Eya1 and Six1 are essential for early steps of sensory neurogenesis in mammalian cranial placodes. Development 131, 5561–5572.

Zou, D., Silvius, D., Davenport, J., Grifone, R., Maire, P., Xu, P.X., 2006. Patterning of the third pharyngeal pouch into thymus/parathyroid by Six and Eya1. Dev. Biol. 293, 499–512.

Zuber, M.E., Perron, M., Philpott, A., Bang, A., Harris, W.A., 1999. Giant eyes in *Xenopus laevis* by overexpression of *Xoptx2*. Cell 98, 341–352.

【腎の発生・発達と腎再生】

Sall familyと腎の発生・幹細胞

Sall family in kidney development

井上秀二(写真)　西中村隆一
Shuji INOUE and Ryuichi NISHINAKAMURA
熊本大学発生医学研究センター細胞識別分野

◎腎は老廃物の排泄や体内の恒常性の維持などの重要な役割を担い，必要不可欠の臓器であるが，自然には再生しない．現在の腎不全治療は多くの問題を抱えており，これに代わる新しい治療法として再生医療が注目を浴びている．腎再生を実現するためには腎の発生を理解することが重要である．本稿では腎の発生機構をおおまかに述べ，Sall1 の腎発生における役割，および Sall ファミリーである Sall4 の機能，さらに Sall1 を使った腎前駆細胞の同定について解説する．

Key word：Sall1，腎発生，ES細胞，再生医療

腎発生の分子機構

腎は中間中胚葉から発生し，前腎，中腎，後腎の3段階を経て形成される．ヒトを含めた哺乳類では前腎と中腎は発生期に退行し，最終的に後腎から腎が形成される[1]．

後腎の発生は後腎間葉と Wolff 管から伸びる尿管芽との相互作用からはじまる．GDNF(glial-cell-line-derived neurotrophic factor)は後腎間葉から分泌される．TGF-β(trans-forming growth factor-β)ファミリーに属する液性因子で，Wolff 管に作用して尿管芽を形成・伸長させる機能をもつ[2]．尿管芽には GDNF の受容体分子である Ret とその共同受容体の Gfra1(GDNF family receptor α1)が発現しており，間葉で分泌された GDNF はこの Ret を介して尿管芽へシグナルを伝える．この GDNF-Ret/Gfra1 シグナルが入らないマウスでは尿管芽が形成されない．また，受容体チロシンキナーゼに抑制的に働く Sprouty1 が Wolff 管に発現しており，GDNF-Ret/Gfra1 シグナルを負に制御している[3]．よって *Sprouty1* のノックアウトマウスでは Wolff 管から複数の尿管芽が形成される．このように GDNF は尿管芽の形成に必須であり，多くの遺伝子の制御によって GDNF が後腎間葉の狭い領域に発現する(図 1-A)．これにより適切な位置に単一の尿管芽が形成されると考えられる．

尿管芽のブランチング

GDNF-Ret/Gfra1 シグナルは，後腎間葉への尿管芽侵入後のブランチング(枝分かれ)でも重要である．また，間質(stroma)も尿管芽のブランチングの制御をしている．間質は枝分かれした尿管芽や凝集した間葉の周辺に発生する組織である．間質ではレチノイン酸受容体 Rara/Rarb(retinoic acid receptor α/β)が共発現しており，尿管芽での Ret の発現を正に制御している[4]．しかし，何の因子が間質から尿管芽へとシグナルを伝えているかは明らかではない．FGF7(fibroblast growth factor)，FGF10 はその候補因子のひとつであり，尿管芽周囲の間質に発現し，尿管芽に発現するレセプター FGFR2b を介して尿管芽の成長・分岐を制御している(図 1-B)．

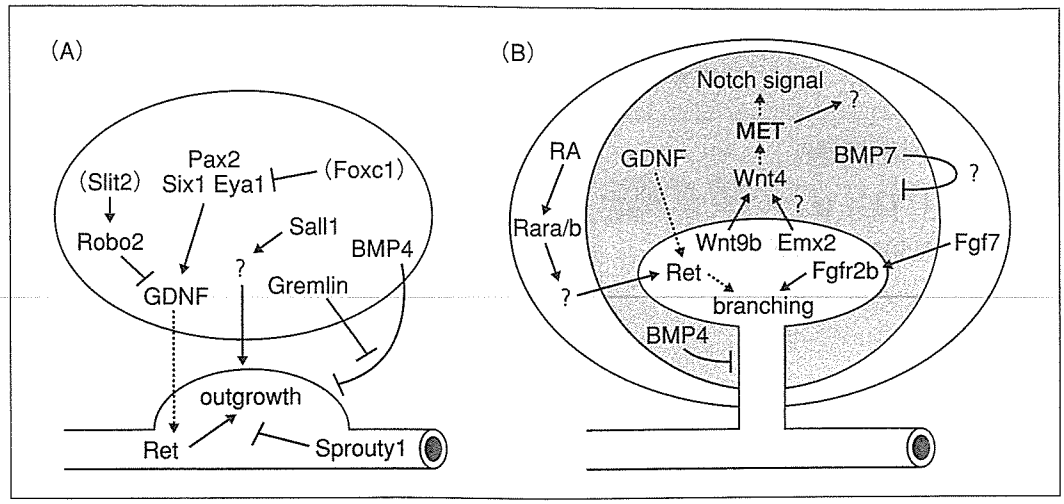

図 1　腎発生における遺伝子の機能(模式図)

A：E10.5 マウス後腎間葉における遺伝子カスケード．( )内の遺伝子は後腎間葉よりも前部の間葉で発現し，異所性の尿管芽形成を抑えている．

B：尿管芽の間葉への侵入後の遺伝子カスケード．

間葉の上皮化(mesenchymal-to-epithelial transformation：MET)

後腎間葉は尿管芽の侵入後に上皮への分化を開始し，糸球体や尿細管へと分化する．これは尿管芽から後腎間葉を上皮化するような誘導物質が分泌されていることが考えられてきた．いままでに LIF(leukemia inhibitory factor)や FGF2, TGF-β などいくつかの候補因子が同定されている．しかし，ノックアウトマウス解析において，その候補因子の多くが腎発生では軽度な表現型しか示さないなかで，尿管芽から分泌される Wnt9b が後腎間葉の MET に必須であるとの報告がなされた．*Wnt9b* のノックアウトマウスでは尿管芽は後腎間葉へ侵入するが，後腎間葉では管腔構造を認めない．MET 後マーカーである Wnt4 や FGF8, Pax8(paired box gene 8)の発現を認めず，MET を起こさないことがわかった[5]．これらより尿管芽から Wnt9b が分泌され，これによって間葉での Wnt4 の発現が誘導される．さらに，Wnt4 は間葉自身に働いて MET が引き起こされることがわかった(図 1-B)．

Sall1は腎発生に必須である

アフリカツメガエル(Xenopus laevis)の胞胚から切り出したアニマルキャップを培養して各種臓器を誘導する系が浅島らにより確立されている(前項参照)．この系ではアクチビンとレチノイン酸の存在下に生理食塩水中で培養すると 3 日後に三次元立体構造をもった前腎管が形成されることが示されている．この *in vitro* 腎誘導系を用い，Zinc フィンガードメインを 8 個もつ蛋白をコードする遺伝子 *Xsal-3* をあらたに単離し，さらにそのマウスホモログである *Sall1* を単離した．*Sall1* はその配列よりヒト *SALL1* のマウスホモログと考えられた．

Sall1 は，尿管芽が後腎間葉に侵入する以前であるマウス胎生 10.5 日から間葉に発現する．胎生 11.5 日以降も尿管芽での発現はみられないが，後腎間葉での強い発現が維持される．Sall1 は腎のほかに，中枢神経系，耳胞，心臓，肢芽，肛門などでの発現を認めるが，そのノックアウトマウスの症状は腎に限局していた．つまり *Sall1* ノックアウトマウスは尿管芽が伸長せず，腎が完全に欠損するか痕跡的であり，Sall1 が腎発生にきわめて重要であることが証明された[6]．しかし，*Sall1* ノックアウトマウスでは GDNF の発現は失われておらず，GDNF のほかに Sall1 が制御する別の機構が存在することを意味している(図 1-A)．

Sall4はES細胞に必須であり，Sall1と協調して腎を形成する

前述のように Sall1 は腎以外でも発現しているにもかかわらず，*Sall1* ノックアウトマウスでは他